Automation, import competition, and intra-household labor supply

Claudio Costanzo*

December 22, 2025

Abstract

This paper examines how industrial automation and import competition—two forces that raise women's wages relative to men's—reshape household time allocation. Linking the American Time Use Survey to commuting-zone exposure to robot adoption and Chinese import penetration, I find that greater exposure is associated with women reallocating time out of market work and into leisure and childcare, while men increase market hours and reduce leisure. These patterns are consistent with hypotheses about identity norms that discourage wives from out-earning their husbands. To quantify the norm's effect on time use, I estimate a household model that imposes a disutility cost when the wife's earnings exceed the husband's; the model replicates nonlinearities in time use and implies that the norm approximately doubles the gender gap in market hours relative to an identity-neutral benchmark.

Keywords: Family norms; Childcare; Labor supply; Relative wages; Robots; Trade.

JEL Codes: J16, J22, J31, D13, O33, F16.

*ECARES, Université Libre de Bruxelles. Contact: claudio.costanzo@ulb.be

1 Introduction

Over recent decades, technological adoption and global integration have reshaped the task content of jobs in advanced economies. As industrial robots diffuse, demand shifts toward cognitive and interpersonal tasks and routine work is displaced (de Vries et al., 2020). Greater exposure to international trade has further compressed manufacturing employment and accelerated the reallocation of labor into services (Autor and Dorn, 2013). These shifts align with long-standing gender differences in occupational sorting: many goods-exposed, at-risk occupations are male-dominated, while a large swath of service employment—comparatively insulated from goods-market competition—skews female. Figure 1 plots the distributions of occupational robot exposure and the probability that an occupation is in a goods-tradable industry.[1] Occupations in the upper-end of the distributions, i.e. high in both automation risk and tradable share, are predominantly male, whereas those in the lower-left are predominantly female.

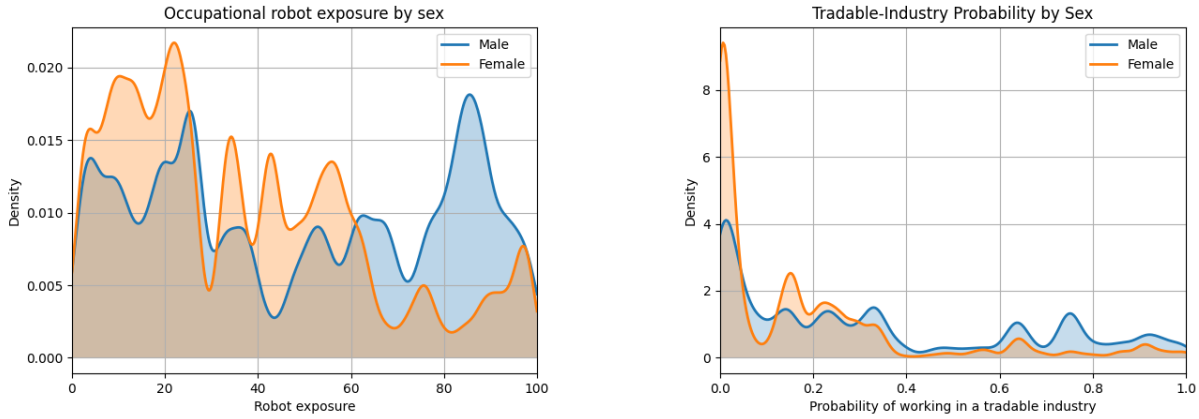

Figure 1: Kernel densities by sex. Source: United States IPUMS Census/ACS microdata, 2000–2020 (Flood et al., 2024). Panel (a) shows the distribution of the robot-exposure score from Webb (2019). Panel (b) shows the distribution of the probability that an occupation is in a goods-tradable industry.

This study traces the consequences of these structural shifts for intra-household time allocation, focusing on how automation and trade expansion, by raising women's relative wages (Ge and Zhou, 2020; Anelli et al., 2021; Besedeš et al., 2021; Autor et al., 2019),

[1] Webb (2019) constructs the robot exposure by measuring the textual overlap between O*NET task descriptions and robot-related patent text. The tradable share is computed as the pooled, person-weighted probability, for each occupation o, that a worker i in o is employed in a tradable industry: $\hat{p}_o = \frac{\sum_{i \in o} w_i \, \mathbf{1}\{\text{Industry}_i \in T\}}{\sum_{i \in o} w_i}$. The set of tradable industries T includes Agriculture/Forestry/Fishing, Mining, Manufacturing; Transport/Communications/Utilities and Wholesale. These different measurement strategies reflects a fundamental distinction: robot exposure is task-based—determined by an occupation's task mix—whereas trade/offshoring exposure is industry-based—determined by whether jobs reside in tradable industries.

reshape the balance between market labor and household production. Unitary and collective models that impose Pareto-efficient household allocations predict that when a spouse's wage rises, that spouse shifts time toward market work and away from home production (Becker, 1965; Gronau, 1977; Chiappori, 1992). A complementary literature argues that social norms and identity concerns can distort these choices, especially when wives approach or surpass husbands' earnings (Bertrand et al., 2015; Bursztyn et al., 2017; Folke and Rickne, 2020).

To understand how changes in the labor market driven by robots and import competition affect households' time use, the empirical design links the American Time Use Survey (ATUS) to commuting–zone measures of exposure to industrial robots and to import competition from China. Both shocks are built as shift–share measures that link historical industry composition in each local labor market with sectoral robot intensity and Chinese import penetration in the US, following Acemoglu and Restrepo (2020) and Autor et al. (2013).

Endogeneity can arise when baseline industry shares correlate with unobserved drivers of time use (e.g., union history, child–care supply, gender norms); when national shifters partly reflect local conditions (e.g., U.S. demand booms raising Chinese exports; tight local labor markets prompting robot adoption); from common industry trends that affect both trade and automation; and from policy confounds. To strengthen identification, I instrument U.S. industry–level robot adoption with contemporaneous changes in European adoption at the same industry level, and U.S. industry–level import penetration from China with Chinese export growth to other high–income markets. Intuitively, these instruments shift households' potential wage shares without directly affecting how couples allocate time.

Greater exposure to either robots or Chinese import competition is associated with a reallocation of time within couples: women reduce market hours and increase time in leisure and childcare, while men increase market hours and reduce leisure. Quantitatively, a one–unit higher stock of robots per 1,000 workers reallocates about one hour per week at the household level across market work, childcare, and leisure. An additional $1,000 of Chinese imports per worker reduces women's market time by roughly three hours per week, with a corresponding rise in childcare. These results point towards hypotheses about social norms that discourage wives from out-earning their husbands: because these shocks disproportionately depress men's earnings in the lower half of the wage distribution, the largest shifts in within-couple wage shares occur in households where women already contribute a relatively high share of income, i.e. where the identity norm is most likely to induce reductions in their market work.

To rationalize the evidence, I build a structural model of household time allocation with shared consumption, child quality as a public good produced by parental time, and leisure as a private good. A penalty term—defined as a function of the wife's earnings relative to the husband's—captures the disutility from violating the breadwinner norm. Parameters

are estimated by the Simulated Method of Moments to match the non-monotonic time–use profiles in the ATUS. The gender gap in time use roughly doubles relative to a model without the norm, rising from 14% to 24% for market work and from 5% to 10% for childcare.

Counterfactuals that reduce the share of low-wage men or increase the share of high-wage women show that, once the norm is introduced, the divergence grows as the gender wage gap narrows. The simulations highlight three facts: (i) the norm induces a kink at the equal-earnings threshold, generating the inverse-U in women's market hours (and the mirror pattern in childcare); (ii) aggregate effects scale nonlinearly with the distribution of relative wages—shifts that move couples beyond parity disproportionately increase the fraction of households for which the norm binds; and (iii) the norm depresses welfare relative to the efficient benchmark by reallocating time away from market work even when wives' market productivity is high.

The paper makes three distinct contributions to the literature. First, it examines how industrial automation and trade reshape family dynamics. Autor et al. (2019) and Anelli et al. (2021) document that these shocks reduce marriage rates while increasing cohabitation and divorce due to a decline in men's marriage-market value. Costanzo (2025) and Keller and Utar (2022) link the two forces to fertility choices. Here, the focus is on how automation and trade alters spouses' joint decision-making over the allocation of their time between market and non-market activities.

Second, by exploiting variation in spouses' relative potential wages induced by the adoption of industrial robots and exposure to import competition, it addresses criticisms made of Bertrand et al. (2015) regarding irregularities in time allocation when spouses' wages converge. On the one hand, Getik (2024) finds that women who outearn their husbands experience a decline in mental health, thus supporting the hypothesis of an anomalous behavior after wage parity; on the other hand, Heggeness and Murray-Close (2019); Rosenberg (2021) warn that reported spousal earnings may be endogenous, with reporting bias especially likely when partners are interviewed jointly. Moreover, Zinovyeva and Tverdostup (2021) argue that the observed discontinuity in couple counts beyond the point of equal earnings reflects a convergence effect—women reduce their work hours to align their earnings with their spouses'. Industrial automation and trade thus serve as exogenous sources of wage variation and change the probability that women become the household's primary earners.

Third, it estimates a structural household time–use model that reproduces the observed non-linear relationship between time allocation and spouses' wage shares. While prior structural time-use models study wage shocks (Blundell et al. 2018) and the link between parental education and childcare time (Gobbi 2018), the framework here captures how shifts in

women's wage shares—such as those driven by automation and trade expansion—reshape the allocation of time between market work, childcare, and leisure.

Section 2 describes the data, sample restrictions, and the construction of the shift–share exposures to robots and Chinese import competition, together with the external instruments. Section 3 lays out the empirical specification and presents OLS and 2SLS estimates for both shocks— including the gender-oriented decomposition of the trade exposure—plus robustness exercises (weekly hours, automotive controls, and AKM shock-level inference). Section 4 first documents stylized facts on wage shares and time use (Section 4.1), then develops and estimates a structural household model with an identity wedge and reports counterfactuals. Finally, Section 5 concludes.

2 Data, sample, and measurement

The main data for the analysis are gathered from the American Time Use Survey (ATUS), the International Federation of Robotics (IFR), and the UN Comtrade Database on U.S. imports.

ATUS sample. ATUS provides nationally representative, diary-based measures of minutes spent on activities over a 24-hour day. The survey has run continuously since 2003, drawing one respondent (age 15+) from households that recently completed the CPS. The analysis sample consists of married or cohabiting households with at least one employed spouse and at least one child aged 10 or younger (following Blundell et al., 2018). Market work corresponds to ATUS "work and work-related activities," childcare to "caring for and helping household children," and leisure to standard leisure categories.

Table 1 provides summary statistics for the sample population, while Appendix Table A1 reports information for the general population. With young children present, couples reallocate time away from leisure and toward childcare: for men, leisure averages 262 minutes/day in the sample vs. 357 minutes in the general population. For women, leisure falls from 310 to 227 minutes. Men in the sample also record more market work time (262 vs. 191 minutes/day), while women's remains stable (132 vs. 127 minutes/day). Consistent with these diary measures, usual weekly hours are higher for men in the sample (44.0 vs. 30.9) and similar for women (23.6 vs. 21.2). The sample is younger and more educated than the general population, while hourly wages are comparable across groups.

Table 1: Descriptive statistics: ATUS analysis sample (households with young children)

	Females			Males		
Variable	Obs	Mean	Std. Dev.	Obs	Mean	Std. Dev.
Leisure (min/day)	24,748	226.80	164.97	22,021	262.00	195.74
Childcare (min/day)	24,748	142.94	147.38	22,021	79.19	113.27
Market work (min/day)	24,748	132.19	215.60	22,021	261.95	277.40
Age	24,748	35.49	6.78	22,021	38.05	7.54
Hourly wage (USD)	7,381	16.45	10.49	7,839	18.68	10.21
Weekly earnings (USD)	14,013	757.96	534.22	16,666	1,086.80	594.43
Usual work hours per week	23,048	23.56	19.61	20,463	44.00	14.24
Less than secondary (%)	24,748	7.85	26.90	22,021	8.72	28.22
Secondary (%)	24,748	19.12	39.33	22,021	22.17	41.54
Some college (%)	24,748	26.54	44.16	22,021	24.83	43.20
Tertiary (%)	24,748	46.48	49.88	22,021	44.28	49.67

Notes: The sample is restricted to married/cohabiting households with at least one employed spouse and at least one child aged $\leq$10. Leisure, childcare, and market work are ATUS diary minutes/day. Hourly wage, weekly earnings, and usual hours come from the linked CPS. Education rows report the share (%) with each attainment category.

Exposure to robots and import competition can affect marriage and fertility (Autor et al., 2019; Anelli et al., 2021), so conditioning on couples with young children may raise selection concerns. This issue is addressed at the end of Section 3.2 suggesting that, under the proposed causal mechanism, any resulting selection would, if anything, attenuate rather than inflate the estimated responses.

Local exposure to robots. Data on the stock of industrial robots at the country–year–sector level are provided by the International Federation of Robotics (IFR), which conducts annual surveys on the number of robots sold in each country across various industries, covering 1993–2019. The IFR defines industrial robots as "automatically controlled, reprogrammable, and multipurpose machines" that are fully autonomous, do not require human operators, and are capable of performing repetitive tasks. The evolution of robots usage in the US is shown in Figure 2. Adoption began to rise markedly around 1990 and kept accelerating thereafter.

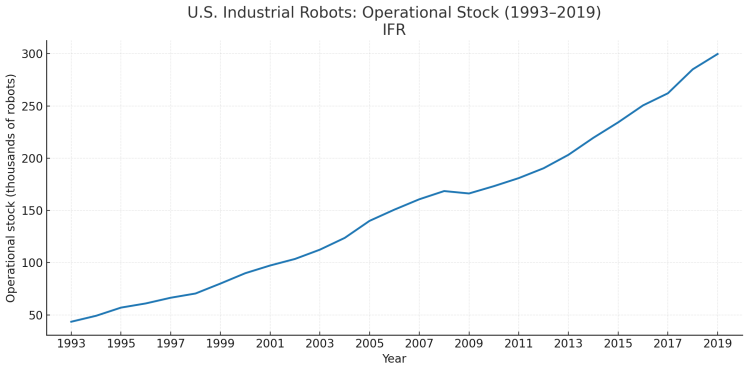

Figure 2: U.S. industrial robot operational stock, 1993–2019 (IFR).

The dataset presents some limitations. Sectoral information for the United States is only available from 2004 onward. While the data for manufacturing industries are detailed, information on other sectors is aggregated. The dataset includes the number of robots used in 13 manufacturing sectors and six non-manufacturing categories: Agriculture and Fishery, automotive, construction, electronics, food, furniture, basic metals, machinery, metal products, mineral, mining, paper, petrochemicals, research, services, textiles, utilities, non-automotive vehicles, and the remaining manufacturing sectors aggregated. Additionally, the dataset only provides data at the country level, lacking finer geographical details within countries.

The explanatory variable measures local labor market exposure to industrial robotics at the commuting-zone level using a Bartik-style instrument, following Acemoglu and Restrepo (2020). This approach assumes a uniform distribution of robots across industries within a commuting zone, exploiting variation in pre-sample local employment distribution by sector and the evolution of robot stocks by sector in the country.

In line with standard shift-share measures, the variable is based on the industrial composition of local labor markets before the surge in industrial automation. By using historical differences in the industrial specializations of regions, it addresses endogeneity concerns arising from the possibility that current employment levels are influenced by the same unobserved factors that drive robot adoption. The historical specialization is represented by the 1990 employment share, retrieved from census data, in the commuting zone. The measure of exposure in a given industry is obtained by multiplying the baseline employment share in the region by the ratio of robots to employed workers in the country.[2] After that, the industry-specific scores are summed to obtain the commuting-zone exposure to industrial robotics:

$$Robots_{ct} = \sum_{s} \frac{Empl_{sc}^{90}}{Empl_{c}^{90}} \frac{StockRobots_{st}}{Empl_{s}^{90}}, \tag{1}$$

[2]Approximately a third of the industrial robots are not classified by sector; these are allocated proportionally based on the classified data, as in Acemoglu and Restrepo (2020).

where the subscripts s, c, and t denote industry, commuting zone, and year, respectively. $Empl_{sc}^{1990}$ represents the number of employed workers in industry s and commuting zone c, and $Empl_{c}^{1990}$ is the total employment in the commuting zone. $\frac{StockRobots_{st}}{Empl_{s}^{1990}}$ denotes the number of robots per thousand workers relative to the 1990 level.

Endogeneity concerns may arise from several sources. For instance, some local labor markets may have stronger employment protection legislation than others, which increases the cost of labor and would incentivize firms to install more robots. This concern is mitigated by including a set of state-year fixed effects, since laws are typically enacted at the state level. However, another possible concern is that certain labor markets may have stronger labor unions locally, which could similarly increase the cost of human labor for firms. In addition, labor supply decisions may be influenced by economic conditions, which are in turn correlated with the adoption of robots in the industry.

To address endogeneity issues, the usage of robots in other European economies is used as an instrument for the adoption in the U.S. The variable is defined as follows:

$$Robots_{ct}^{IV} = \frac{1}{5} \sum_{j \in EU5} \left(\sum_{s} \frac{Empl_{sc}^{70}}{Empl_{c}^{70}} \frac{StockRobots_{st}^{j}}{Empl_{s}^{j,90}} \right), \tag{2}$$

where $j \in EU5$ refers to Denmark, Finland, France, Italy, and Sweden. These countries are ahead of the U.S. in the use of robots[3]. The instrument involves multiplying the historical industrial specialization of the labor market in 1970, to avoid mechanical correlation with any pre-1990 robot adoption, by the penetration of robots in the same industry per thousand workers in the European country j in the baseline year. The number of workers in 1990 for the five European countries is retrieved from EUKLEMS (van Ark and Jäger 2017). The instrument is designed to exploit common industry-specific trends in automation, driven by shared technological innovations between countries. Since there are few international companies that provide industrial robots and, hence, drive the global trend in automation, we can reasonably assume the relevance of $Exposure_{ct}^{IV}$. Validity requires that European industry–level automation affects U.S. time use only via its impact on U.S. robot adoption—i.e., not through concurrent global industry shocks, trade linkages, or macro conditions after controls and fixed effects.

Local exposure to import competition. Following the extensive literature on trade shocks, exposure to import competition is measured by the rise in imports from China. The

[3]Germany is the leading country in terms of automation. It is excluded from the construction of the instrument because it is far ahead of the other countries and may not be as relevant to U.S. patterns as the EU5.

focus on China stems from its role in the expansion of U.S. imports from low-income countries since the early 1990s, driven by market reforms, large-scale rural-to-urban migration, and enhanced access to foreign technology and capital. These domestic transformations, together with China's accession to the WTO—which granted it most-favored-nation status—have markedly increased its export capacity. Over time, imports from China began rising in the 1990s, then entered a phase of exponential growth starting with its 2001 WTO accession, and finally leveled off in 2014, as shown in Figure 3.[4]

Figure 3: U.S. goods imports from China, 1990–2024 (Census basis, nominal).

Autor et al. (2013) extract annual bilateral export flows from China by product to the United States and to other high-income destinations. Product-level values are mapped to U.S. industries using standard NAICS concordances and aggregated to construct industry-level Chinese import exposure.

Using information on U.S. imports from China, domestic absorption, and local labor market sectoral employment, the trade liberalization shock takes the following shift-share form:

$$\text{Trade}_{ct} = \sum_{s} \left(\frac{Empl_{sc,90}}{Empl_{c,1990}} \right) \frac{\text{Import}_{st}^{Ch \to US}}{Domestic\,Absorption_{s,90}} \tag{3}$$

where employment shares across 397 four-digit SIC manufacturing industries are multiplied by the dollar amount of imports from China in the U.S., divided by the domestic production in the sector.

Bias can arise if baseline industry shares correlate with slow-moving local traits (union strength, child-care supply, gender norms); if shifters reflect U.S.-specific conditions (demand booms, offshoring by multinationals, tariff changes); or from anticipation and policy timing. To address endogeneity concerns, an instrumental variable is constructed by substituting U.S. import penetration from China with the industry-level growth of Chinese exports to

[4]The ATUS sample when investigating the effect of import com[petition therefore spans 2003-2014.

eight other developed countries.[5] Formally:

$$\text{Trade}_{ct}^{iv} = \sum_{j} \left(\frac{Empl_{sc,80}}{Empl_{c,80}} \right) \frac{\text{Import}_{st}^{Ch \to Others}}{Domestic\,Absorption_{s,90}}. \tag{4}$$

Baseline employment shares are taken from an earlier year with respect to the early 1990s surge in Chinese exports and any contemporaneous U.S. industry reallocation, to reduce mechanical correlation between the weights and the shift. The instrument uses Chinese exports to other high-income destinations to isolate supply-driven variation; validity requires that, conditional on controls and fixed effects, these foreign export surges affect U.S. time use only through U.S. import competition, not via global industry shocks or re-routing unrelated to U.S. demand.

Decomposing the trade shock. Whereas industrial automation differentially affects wages and employment according to task content, trade shocks vary in intensity across sectors. This distinction allows us to break down the overall trade exposure into components that are more pronounced in female- or male-dominated industries. To do so, we can introduce an extra dimension of variation: the historical female share of employment in each industry–commuting-zone pair, $f_{cs,90}$, and its complement, $1 - f_{cs,90}$. We can therefore express the overall exposure as the sum of shocks weighted by these gender-industry shares, yielding the following decomposition:

$$\text{Trade}_{ct}^{g} \;=\; \sum_{s} s_{cs,90}^{g} \left(\tfrac{Empl_{cs,91}}{Empl_{c,1991}} \right) \frac{\text{Import}_{st}^{Ch \to US}}{Domestic\,Absorption_{s,91}}, \quad g \in \{f, m\},$$

where

$$s_{cs,90}^{f} = f_{cs,90}, \quad s_{cs,90}^{m} = 1 - f_{cs,90},$$

denoting trade shocks that comparatively decrease wages for women and men, respectively. The instrumental variable is constructed analogously as the main measure.

Descriptive statistics for local exposures Table 2 reports summary statistics for the two shift–share measures. Robot exposure has a mean of 3.218 (SD 4.122); by construction, one unit corresponds approximately to one additional robot per 1,000 workers (shift–share aggregated). Trade exposure has a mean of 0.006 and a standard deviation of 0.01. Because it is an import-penetration ratio, a value of 0.01 corresponds to a one–percentage–point increase in Chinese import penetration.

[5] Namely: Australia, Denmark, Finland, Germany, Japan, New Zealand, Spain, and Switzerland.

Table 2: Summary statistics of robot and trade shift-share measures.

Variable	Mean	Std. Dev.	Min.	Max.	N
Robots	3.218	4.122	0.816	33.704	80635
Trade	0.006	0.01	0	0.163	168414

3 The effect of robots and trade on time use

This section describes the pooled cross-section model used to examine the relationship between the exposure to automation and trade with household time use choices. It then presents the OLS and 2SLS[6] results and robustness checks.

3.1 Empirical model

The baseline specification is:

$$Y_{ict} = \alpha + \beta \, \text{Exposure}_{ct} + \eta' C_{ict} + \gamma_c + \delta_{s(c)\times t} + \varepsilon_{ict}, \tag{5}$$

where Y_{ict} represents minutes/day in market work, leisure, and childcare spent by individual i; Exposure_{ct} is the shift–share measure (robots or trade) for commuting zone c in year t; and C_{ict} includes temporal, demographic, and economic controls (day of week, month, holiday; number of children; respondent's and spouse's age and education; indicators for children under 5; ages of youngest and oldest child; and family–income category).[7] γ_c are commuting–zone fixed effects and $\delta_{s(c)\times t}$ are state–by–year fixed effects. β represents the change in T for one additional robot per 1,000 workers in the robots specification, and the change in T for a one–unit increase in Chinese import penetration in the trade specification (so a 1 p.p. increase implies $0.01\,\beta$). Regressions use ATUS survey weights and standard errors are clustered at the commuting–zone–year level. Active job seekers (unemployed and looking for a job) are excluded in order to reduce the bias driven by unemployment effects of the shocks.

To address endogeneity, I estimate two–stage least squares (2SLS), instrumenting Exposure_{ct} with its external shifter:

$$\text{Exposure}_{ct} \;=\; \pi \, \text{Exposure}^{IV}_{ct} + \gamma_c + \delta_{s(c)\times t} + u_{ct}, \tag{6}$$

which yields the fitted value $\widehat{\text{Exposure}}_{ct}$. The second stage replaces the endogenous regressor

[6] Throughout the 2SLS analyses, the Kleibergen and Paap (2006) F-Statistics hover around a value of 300.

[7] Family income in ATUS is categorized into 16 levels from less than \$5,000 to \$150,000 and over.

with this fitted value:

$$Y_{ict} = \alpha + \beta \widehat{\text{Exposure}}_{ct} + \eta' C_{ict} + \gamma_c + \delta_{s(c)\times t} + \varepsilon_{ict}. \tag{7}$$

3.2 Results

This section reports estimation results. The estimates are reported on three subsamples defined by spouses' employment: households in which the spouse of the respondent works, households in which the respondent works, and households in which both spouses work. This setup allows me to consider both intensive and extensive margins in time allocation. Each table reports *OLS* and *2SLS* estimates; in the latter, Exposure_{ct} is instrumented with the corresponding external shifter (EU5 industry robot adoption for robots; Chinese exports to other high-income destinations for trade).[8]

Exposure to robots. Table 3 shows the response of daily time use to a one–unit increase in robot exposure (roughly one additional robot per 1,000 workers, shift–share aggregated). For men, market work rises by about 14 minutes when including corner solutions (column 1), by 7–8 minutes for respondent–employed individuals (column 2), and by 16–18 minutes in two–earner households (column 3), with slightly larger magnitudes in 2SLS. Men's leisure falls by 10–12 minutes in two–earner households. For women, market work declines by about 10–15 minutes per day. On the intensive margin, childcare rises by about 4–5 minutes in OLS and about 8 minutes in 2SLS (columns 5–6). Leisure increases for women by about 7–11 minutes. Given the exposure standard deviation of about 4, a one–standard–deviation increase scales these per–unit effects by roughly four.

Overall, robot exposure reallocates time within couples: women shift out of market work into childcare and leisure, while men shift into market work (and out of leisure), especially in two–earner households. 2SLS estimates are typically larger in absolute value than OLS, consistent with attenuation or endogenous adjustments that bias OLS toward zero.

[8] First-stage strength is high throughout (Kleibergen–Paap $F \approx 300$).

Table 3: Effect of robots on time spent working, childcaring, and leisuring per day.

	Males			Females		
	(1)	(2)	(3)	(4)	(5)	(6)
Daily minutes work						
Robots	14.06***	6.633*	16.06***	-9.726**	-13.05***	-10.74**
	(4.669)	(3.421)	(5.409)	(3.883)	(4.471)	(4.910)
Robots^{2SLS}	13.92**	8.376*	18.02**	-15.40***	-18.76***	-15.26**
	(6.598)	(4.618)	(7.384)	(5.073)	(5.899)	(6.628)
Observations	6,795	6,582	3,905	7,668	4,974	4,546
R-squared	0.426	0.455	0.529	0.297	0.430	0.476
Daily minutes childcare						
Robots	-0.490	0.703	-0.407	1.988	4.624**	4.912**
	(1.818)	(1.417)	(1.900)	(2.019)	(1.963)	(2.434)
Robots^{2SLS}	0.160	1.687	-0.773	5.579*	8.220***	8.455**
	(2.533)	(2.111)	(2.707)	(2.975)	(2.701)	(3.383)
Observations	6,795	6,582	3,905	7,668	4,974	4,546
R-squared	0.170	0.179	0.323	0.230	0.232	0.290
Daily minutes leisure						
Robots	-4.724*	-3.646	-9.912***	7.247***	9.145***	8.891***
	(2.663)	(2.699)	(3.449)	(2.159)	(2.389)	(2.789)
Robots^{2SLS}	-4.019	-3.869	-11.87***	7.214**	10.13***	10.67***
	(3.400)	(3.365)	(3.818)	(2.968)	(3.186)	(3.918)
Observations	6,795	6,582	3,905	7,668	4,974	4,546
R-squared	0.251	0.262	0.362	0.215	0.310	0.353
Spouse employed	✓		✓	✓		✓
Respondent employed		✓	✓		✓	✓

Sample: married or cohabiting couples with at least a spouse working and children aged 10 or less. Control variables in all specifications include state∗year-level fixed effects, spouses' age and education, number of children (total and under age 5), ages of the youngest and oldest child, family-income classification, day-of-week and month-of-survey fixed effects, and a holiday indicator. Standard errors clustered at the commuting-zone–year level are in parentheses. *** $p < 0.01$, ** $p < 0.05$, * $p < 0.1$.

Exposure to trade. Table 4 reports effects of Chinese import competition. Coefficients are per unit of the import–penetration ratio; per one percentage point effects correspond to 0.01 the coefficient, as the trade exposure is a ratio in 0–1 units. For men, a 1 pp increase reduces daily work time by about 32–41 minutes in OLS and about 51–65 minutes

in 2SLS (columns 1–3). For women, work time falls on the intensive margin by about 27–33 minutes in OLS (columns 5–6) and by about 29 minutes in 2SLS (column 6), while the spouse–employed sample (column 4) shows a small positive OLS effect (about 10 minutes per 1 pp). Childcare moves in the same direction as in the robot analysis: on the intensive margin, women devote about 14–22 minutes per 1 pp more to childcare (OLS columns 5–6; 2SLS column 6). Leisure shows no consistent pattern, apart from a modest decline for women whose spouses are employed (2SLS, column 4, around 15 minutes per 1 pp).

Unlike robots, the China shock depresses market time for both spouses on the intensive margin. Women substitute toward childcare as market work falls. 2SLS magnitudes exceed OLS, again suggesting attenuation or endogenous adjustments in OLS.

Table 4: Effect of China shock on time spent working, childcaring, and leisuring per day.

	Males			Females		
	(1)	(2)	(3)	(4)	(5)	(6)
Daily minutes work						
Trade	-4,108***	-3,364**	-3,221***	1,015	-2,648**	-3,343***
	(1,263)	(1,711)	(1,115)	(1,020)	(1,257)	(1,208)
$\text{Trade}^{\text{2SLS}}$	-6,464***	-5,944**	-5,106***	1,907	-2,062	-2,940**
	(1,809)	(2,391)	(1,550)	(1,192)	(1,380)	(1,433)
Observations	3,507	5,726	3,305	6,324	4,300	3,899
R-squared	0.431	0.431	0.512	0.272	0.402	0.460
Daily minutes childcare						
Trade	876.3	904.7	633.2	-379.3	1,356**	2,170***
	(796.8)	(887.9)	(774.1)	(563.3)	(665.8)	(670.7)
$\text{Trade}^{\text{2SLS}}$	1,127	2,054	605.2	138.9	967.3	2,067**
	(873.1)	(1,477)	(825.9)	(656.8)	(795.3)	(853.1)
Observations	3,507	5,726	3,305	6,324	4,300	3,899
R-squared	0.225	0.171	0.316	0.227	0.226	0.283
Daily minutes leisure						
Trade	-1,267	8.253	-955.6	-748.3	-27.14	385.9
	(913.7)	(1,012)	(949.0)	(736.8)	(793.3)	(952.5)
$\text{Trade}^{\text{2SLS}}$	-389.9	469.2	-168.8	-1,453*	-784.9	-362.8
	(1,145)	(1,200)	(1,235)	(869.9)	(977.6)	(1,112)
Observations	3,507	5,726	3,305	6,324	4,300	3,899
R-squared	0.312	0.270	0.378	0.208	0.289	0.338
Spouse employed	✓		✓	✓		✓
Respondent employed		✓	✓		✓	✓

Sample: married or cohabiting couples with at least a spouse working and children aged 10 or less. Control variables in all specifications include state∗year-level fixed effects, spouses' age and education, number of children (total and under age 5), ages of the youngest and oldest child, family-income classification, day-of-week and month-of-survey fixed effects, and a holiday indicator. Standard errors clustered at the commuting-zone–year level are in parentheses. *** $p < 0.01$, ** $p < 0.05$, * $p < 0.1$.

Gender–oriented trade shocks. Table 5 decomposes exposure by historical gender intensity. By construction, Trade_{Male} loads on male-dominated industries and lowers men's wages relative to women's (raising women's relative wage), mirroring the direction of the robot shock; conversely, Trade_{Fem} loads on female-dominated industries and lowers women's

wages relative to men's. Focusing on coefficients that are statistically significant in both OLS and 2SLS, the robust patterns are concentrated on men: under Trade_{Male}, male leisure falls by about 173 to 176 minutes per day per one percentage point in the spouse-employed and two-earner samples. Under Trade_{Fem}, male work falls by roughly 212 to 343 minutes per day per one percentage point, and male leisure rises by about 216 to 256 minutes per day per one percentage point. With a standard deviation of about 0.01, a one standard deviation change corresponds approximately to the per percentage point numbers reported. Female coefficients are smaller and typically not jointly significant across OLS and 2SLS.

Table 5: Effect of China shock on time spent working, childcaring, and leisuring per day.

	Males			Females		
	(1)	(2)	(3)	(4)	(5)	(6)
Daily minutes work						
Trade_{Male}	11,834**	7,191**	12,396**	3,715	1,100	-930.8
	(5,204)	(3,529)	(5,054)	(3,301)	(5,077)	(4,886)
$\text{Trade}^{\text{2SLS}}_{Male}$	12,104	3,581	8,834	3,027	-1,340	-4,278
	(8,036)	(5,805)	(7,418)	(5,362)	(7,632)	(8,164)
Trade_{Fem}	-30,002***	-21,226***	-30,241***	-3,601	-9,162	-7,905
	(7,940)	(6,127)	(7,971)	(5,279)	(8,447)	(8,484)
$\text{Trade}^{\text{2SLS}}_{Fem}$	-34,282***	-20,546**	-27,758**	-476.7	-3,874	-1,475
	(12,443)	(9,692)	(12,004)	(8,515)	(12,102)	(13,134)
Daily minutes childcare						
Trade_{Male}	100.0	1,270	1,793	1,050	1,695	2,479
	(2,873)	(1,844)	(2,793)	(1,925)	(1,949)	(2,182)
$\text{Trade}^{\text{2SLS}}_{Male}$	6,228	4,300	7,127*	-2,684	-1,603	-2,293
	(3,924)	(2,843)	(3,655)	(3,261)	(3,590)	(4,392)
Trade_{Fem}	2,026	174.6	-1,326	-2,471	987.8	1,826
	(4,039)	(2,602)	(4,036)	(2,982)	(3,573)	(3,963)
$\text{Trade}^{\text{2SLS}}_{Fem}$	-6,492	-1,309	-9,280	4,910	5,079	8,939
	(5,678)	(4,613)	(5,695)	(5,229)	(5,832)	(7,029)
Daily minutes leisure						
Trade_{Male}	-17,278***	-6,121**	-17,629***	-4,089	-1,090	-1,633
	(3,547)	(2,538)	(3,437)	(3,217)	(3,170)	(3,502)
$\text{Trade}^{\text{2SLS}}_{Male}$	-17,611***	-5,883	-14,711***	-809.3	2,043	426.1
	(5,484)	(3,835)	(5,416)	(4,216)	(4,775)	(5,188)
Trade_{Fem}	24,825***	10,479**	25,588***	4,590	1,679	3,201
	(5,888)	(4,448)	(5,819)	(5,433)	(5,689)	(6,094)
$\text{Trade}^{\text{2SLS}}_{Fem}$	25,302***	10,115	21,618**	-2,451	-5,012	-1,888
	(8,742)	(6,177)	(8,664)	(6,495)	(7,639)	(8,234)
Spouse employed	✓		✓	✓		✓
Respondent employed		✓	✓		✓	✓

Sample: married or cohabiting couples with at least a spouse working and children aged 10 or less. Control variables in all specifications include state∗year-level fixed effects, spouses' age and education, number of children (total and under age 5), ages of the youngest and oldest child, family-income classification, day-of-week and month-of-survey fixed effects, and a holiday indicator. Standard errors clustered at the commuting-zone–year level are in parentheses. *** $p < 0.01$, ** $p < 0.05$, * $p < 0.1$.

Causal mechanism and selection. An interpretation of these dynamics is that they arise from the interaction of (i) the skewed incidence of robot and trade shocks on wages and (ii) family identity norms. Exposure to automation and import competition disproportionately compresses men's earnings in the lower–middle of the male wage distribution. This implies that a large share of the affected couples already sit at or just beyond parity, where breadwinner norms are most likely to bind (Bertrand et al., 2015; Getik, 2024). In this region, increases in women's relative earnings translate into asymmetric time reallocation: women reduce market hours and increase childcare and leisure, while men exhibit the mirror adjustment.

An alternative explanation is that these shocks operate through a purely technological channel: labor-saving innovations or increased import penetration may reduce the number of worker-minutes required to produce a given level of output. Under this mechanism, one would expect to see shorter market hours and offsetting increases in leisure even among individuals without a co-resident partner, since the change in time requirements would be independent of household structure. Appendix Table A4 provides evidence against this interpretation. For individuals not in a relationship, the estimated effects on market and leisure time are close to zero, suggesting that the main results are not driven by generalized reductions in the time intensity of work tasks but rather by intra-household responses to relative earnings shifts.

A concern relates to selection into the estimation sample. The main analysis is restricted to couples with young children, but marriage margins are themselves affected by these shocks, as lower men's wages relative to women's reduce their marriage-market value (Autor et al., 2019; Anelli et al., 2021). The drop in frequency of marriages after the wage equality point is clearly shown in Appendix Figure A1. However, under the identity-norm mechanism, such selection should attenuate rather than exaggerate the estimates. If exposure reduces marriage among lower-earning men—precisely the group whose partners would be most likely to surpass them in relative earnings—then high-exposure local labor markets will contain fewer couples in which breadwinner norms would be expected to bind strongly. Conditioning on families with young children therefore removes many of the highest-intensity cases, implying that the estimated coefficients understate rather than overstate the magnitude of the underlying mechanism.

3.3 Robustness

The following robustness checks address some criticalities that may arise in the main specification.

Weekly hours worked ATUS diaries capture a single day and feature many zero–work diaries (e.g., full-time workers sampled on a day off), which raises outcome noise and makes estimates sensitive to functional-form assumptions in the presence of corner solutions (Hamermesh et al., 2005; Stewart, 2013). To verify that the findings are not an artifact of this one-day snapshot, Table A5 re-estimates the baseline using respondents' *usual weekly hours at the main job* from the CPS interview that precedes the ATUS—a measure that averages over day-to-day variation and exhibits far fewer zeros. Because usual hours are collected for workers, these regressions condition on employment; results are similar when aligning the diary sample accordingly. The coefficients remain tightly aligned with the diary-based estimates—if anything, slightly larger in magnitude: a one-unit increase in robot exposure reduces women's working time by about one hour per week, on average; a one–standard-deviation increase in the China-shock regressor is associated with roughly four fewer hours per week for women. In the decomposed trade specifications, the male-oriented shock raises men's weekly hours by about 7 hours per standard-deviation increase, whereas the female-oriented shock lowers men's hours by about 12 hours, consistent with the within-household reallocation documented above.

Accounting for the automotive industry A common concern with shift–share measures of robot exposure, emphasised by Goldsmith-Pinkham et al. (2020), is that their variation may be driven by sector-specific trends, potentially undermining causal interpretation. The vehicle sector is especially problematic, because the automotive industry has been the largest adopter of robots across the US.[9] Appendix Table A6 reports the Rotemberg weights used to construct the Bartik measure and shows that the vehicle sector receives a disproportionately large weight compared with other industries.

To address the issue, Table A7 in the appendix re-estimates the models after excluding the automotive sector from the exposure variable and entering it separately as a control, following Acemoglu and Restrepo (2020). The loss of variation reduces statistical power for most coefficients, yet the qualitative pattern of the results is unchanged. The OLS estimates indicate that men's working time increases by roughly 40 minutes per day at the intensive margin, while both OLS and 2SLS show a decline in their childcare time of about 15 minutes and 30–40 minutes per day, respectively, for a unit increase the regressor. For leisure, the OLS estimates imply an equivalent reduction for men, whereas the 2SLS estimates suggest an increase for women at the intensive margin.

Appendix Table A8 adjusts for commuting zone-specific trends across quartiles of em-

[9]See Figure 2 in Acemoglu and Restrepo (2020) on the faster rise in robot penetration in this sector relative to other industries in both the US and European labor markets between 1993 and 2007.

ployment share in the vehicle sector. The coefficients remain consistent with the primary findings, with a slight decrease in statistical significance for the intensive margin of work on the women's side.

Shock-based standard errors (AKM). In a Bartik design, all individuals in a commuting zone (CZ) share the same exposure, a weighted combination of sector-year shocks. Clustering at the CZ level can miss correlation induced by common shocks, especially when CZ sizes differ. The AKM1 estimator treats shocks as the sampling units: it allows arbitrary dependence within a sector and assumes independence across sectors Adão et al. (2019).

Let i index individuals, s sectors, and j Bartik regressors. Let w_{is} be the pre-sample employment share of sector s in individual i's CZ. Denote sampling weights by v_i, to distinguish them from shares w_{is}.

Step (I): residualization. Estimate the main specification (OLS or 2SLS) with the full set of controls and fixed effects, using weights v_i if applicable. Save outcome residuals $\hat{e}_i$. For each Bartik regressor x_{ji}, compute the residual $\ddot{x}_{ji}$ from regressing x_{ji} on the same controls and fixed effects (weighted if used in the main specification).

Step (II): weighting. Define $u_{yi} = \sqrt{v_i}\,\hat{e}_i$ and $\tilde{x}_{ji} = \sqrt{v_i}\,\ddot{x}_{ji}$. Form the weighted share matrix $\tilde{W}$ with entries $\tilde{w}_{is} = \sqrt{v_i}\,w_{is}$.

Step (III): collapse to the shock level. Project the residualized Bartik regressor onto the shock space,

$$\hat{X}_{js} = \left[(\tilde{W}'\tilde{W})^{-1}\tilde{W}'\tilde{x}_j\right]_s,$$

and aggregate outcome residuals to shocks,

$$R_s = \sum_i \tilde{w}_{is}\,u_{yi} = \sum_i v_i\,w_{is}\,\hat{e}_i.$$

Step (IV): AKM1 variance. For a single Bartik regressor j,

$$\widehat{\mathrm{Var}}(\hat{\beta}_j) = \frac{\sum_s \left(\hat{X}_{js}\,R_s\right)^2}{\left(\sum_i \tilde{x}_{ji}^2\right)^2}, \qquad \mathrm{SE}_j = \sqrt{\widehat{\mathrm{Var}}(\hat{\beta}_j)}.$$

This is a shock-level EHW estimator: within-sector correlation is unrestricted; shocks are assumed independent across s.

2SLS with one endogenous regressor and one Bartik instrument. Let $\hat{\alpha}$ be the 2SLS coefficient, m_i the endogenous regressor, and $\ddot{m}_i$ its residual after partialing out the controls (weighted). Replace u_{yi} with the structural residual $u_{\Delta i} = \sqrt{v_i}\,(Y_i - \hat{\alpha}\,m_i)$ when forming R_s.

Define the first-stage slope

$$\hat{\beta}_{\mathrm{FS}} = \frac{\sum_i \tilde{x}_{ji}\, \ddot{m}_i}{\sum_i \tilde{x}_{ji}^2}.$$

The standard error for $\hat{\alpha}$ is

$$\mathrm{SE}(\hat{\alpha}) = \frac{\sqrt{\sum_s (\hat{X}_{js} R_s)^2}}{|\hat{\beta}_{\mathrm{FS}}| \sum_i \tilde{x}_{ji}^2}.$$

AKM standard errors for the robot exposure. Applying the AKM estimator of Adão et al. (2019) to the robot exposures leaves the qualitative patterns intact. In Table A9, men's work remains positive and statistically significant in OLS across samples, while men's leisure remains negative and significant in OLS. For women, work remains negative and significant in both OLS and 2SLS, and leisure remains positive and significant in OLS and in 2SLS. For childcare, women's intensive–margin effects are robust: OLS shows increases of 4.62 to 4.91 minutes per day (columns 5–6), and 2SLS shows 8.45 minutes per day (column 6). By contrast, most male 2SLS coefficients are not statistically different from zero under AKM (for work in columns 1–2 and for leisure in columns 1–2), reflecting the more conservative shock–level inference. Overall, AKM confirms a within–household reallocation toward more male market work and less male leisure, and toward less female market work with offsetting increases in female childcare and leisure, while indicating lower 2SLS precision when inference is based on sectoral shocks.

AKM standard errors for the decomposed trade exposure. Using AKM1 shock-level inference for the gender-oriented trade measures leaves most dynamics consistent with the reference estimation, with statistical significance more strong compared to Table 5. Results for work and leisure largely match the expected gender contrast, while childcare moves in the opposite direction under 2SLS.

When looking at Trade_{Male}, for men, work rises and leisure falls in all samples, both OLS and 2SLS. For women, 2SLS shows work falling in two of three samples (columns 5–6) and rising in one (column 4); leisure rises in two of three samples (columns 5–6) but falls in one (column 4). OLS for women moves the other way (work mostly increases and leisure falls), so the clearest support comes from 2SLS. For childcare, 2SLS shows the opposite of the proposed mechanism: men's childcare rises and women's falls across all samples; OLS has weaker and mixed patterns. Magnitudes generally favor the gender contrast even when signs disagree within a sample: male effects on work and leisure are much larger than female effects, so the net reallocation still align with the main results.

In the case of Trade_{Fem}, for men, work falls and leisure rises across all samples and estimators. For women, leisure falls in all three 2SLS specifications (columns 4–6), in line with the hypothesis, but work does not increase: it is near zero in one case and negative in

the other two (both OLS and 2SLS). Childcare again goes against the proposed mechanism under 2SLS: men's childcare falls and women's rises in all samples, while OLS mostly shows increases for both. The relative magnitudes are informative even when signs match across genders: the decline in men's work under Trade_{Fem} is large compared to the smaller decline for women.

Representativeness of the ATUS Sample: Wage Regressions A potential concern in using the American Time Use Survey (ATUS) to study the impact of trade and technology shocks is the relatively smaller sample size and specific coverage compared to the Decennial Census or the American Community Survey (ACS) typically used in the literature (e.g., Autor et al. (2013), Acemoglu and Restrepo (2020)). If the labor market effects of robotization or trade within the ATUS sample deviate significantly from established findings, it would imply that our main results on time allocation might be driven by sample selection specificities rather than general equilibrium adjustments.

To validate the representativeness of our sample, we replicate standard Commuting Zone (CZ) level wage regressions using our aggregated ATUS microdata. We estimate the following model:

$$\Delta \ln w_{ct} = \beta' \cdot \Delta \mathbf{Exposure}_{ct} + \mathbf{X}'_{c,1990}\gamma + \delta_t + \epsilon_{ct} \tag{8}$$

where $\Delta \ln w_{ct}$ is the change in the average log hourly wage for men or women in commuting zone c over period t (3 and 10 years, capturing short-run and long-run adjustments, respectively). The term $\Delta \mathbf{Exposure}_{ct}$ represents the vector of structural shocks. For automation, this corresponds to the change in robot exposure. For trade, the vector of gender-specific trade exposures $(\Delta \text{Trade}^m, \Delta \text{Trade}^f)$ is included, capturing import competition weighted by the historical male and female employment shares within industries. The vector $\mathbf{X}_{c,1990}$ includes the standard set of 1990 baseline controls: demographics, education levels, and industry shares. All regressions are weighted by the ATUS population weights aggregated to the CZ level and include period fixed effects δ_t.

I employ a **stacked long-difference** specification rather than a standard annual two-way fixed effects approach. This choice is motivated by two factors. First, consistent with the trade and automation literature, local labor markets adjust to structural shocks over the medium-to-long run. Annual wage data is subject to transitory fluctuations and business cycle noise that can obscure the structural impact of robot adoption or import penetration (Autor et al., 2013; Acemoglu and Restrepo, 2020). Second, and specific to the ATUS, the sample size is significantly smaller than the Census or ACS. When disaggregated to the CZ level, annual observations can yield cells with few respondents, leading to substantial

measurement error in the dependent variable. Using short-term differences would exacerbate attenuation bias due to high sampling error. Relying on stacked differences over 3 and 10 years smooths out high-frequency sampling noise and isolate the structural variation necessary to identify the causal effects of the shocks.

Tables A2 and A3 present the results for the 3-year and 10-year differences. While the smaller ATUS sample size yields larger standard errors than canonical Census-based studies, the estimated effects are mostly consistent with the established literature regarding the displacement effects of structural shocks.

Table A2 reports the results for robot exposure. In the short run (3-year difference), we find a statistically significant and economically meaningful negative effect of robotization on male wages. Consequently, we observe a narrowing of the gender wage gap in the short run. Over the longer 10-year horizon, estimates become attenuated and statistically insignificant, likely reflecting the reduced sample size available for long-difference calculations in the ATUS panel.

Table A3 presents the results for trade exposure. Here, the dynamics differ: while short-run estimates are noisy, we detect significant effects in the long run (10-year difference), consistent with the view that trade adjustments materialize over medium-to-long horizons (Autor et al., 2013). Specifically, exposure to import competition in female-intensive industries (ΔTrade^f) leads to a significant decline in female wages and a corresponding increase in the gender wage gap. While the coefficients for male-specific trade exposure differ in sign, they lack statistical precision.

In summary, despite the inherent power limitations of the ATUS subsample, the estimates do not diverge from the patterns typically found using broader Census or ACS data. We observe that labor demand shocks exert downward pressure on the wages of exposed groups—men in the case of automation, and women in the case of import competition.

The next section proposes formalization of the causal intuition through a structural model of intra-household decisions, with parameters estimated by matching ATUS data on time use.

4 A structural household model of time use

Starting from showing stylized facts on nonlinearities between women wage shares and households' time use as a potential mechanism, along with the non-uniform distribution of robot and trade shock along the wage distribution, for the findings in Section 3. This section elaborates a collective household model to reproduce the kink in time allocation and formalize the causal intuition of the empirical results. Individuals choose how much time to allocate

to market work, leisure, and childcare in a model based on the semi-cooperative framework of Gobbi (2018).

4.1 Stylized facts on wage shares and time use

This section presents descriptive evidence on how relative wages shape household time allocation. When a woman's share of total household wages surpasses her partner's, both spouses reallocate their time between work, childcare, and leisure in distinct ways. Appendix Section C shows tht ISSP data reveal that this non-monotonic pattern extends to family-oriented beliefs. Finally, on the basis of these stylized facts, the section explores a potential causal mechanism underlying the empirical patterns documented in Section 3.

Data from the ATUS are used to examine the relationship between spouses' wage shares and household time allocation. The sample is restricted to married or cohabiting couples under age 64 with at least one child aged ten or younger. Following Bertrand et al. (2015), hourly wages are calculated by dividing weekly earnings by weekly hours worked[10]. For non-workers, a potential wage is imputed as the mean wage of employed individuals sharing the same education level, five-year age bracket, state of residence, and survey year. Including non-workers permits consideration of adjustments on both the intensive and extensive margins of labor supply.

Figure 4 plots average daily minutes spent working, providing childcare, and engaging in leisure against a wife's wage share[11], with separate linear trends fitted on either side of the parity point. As the wife's wage share rises toward parity, her working time increases up to 0.5 and then declines, while childcare—and, to a lesser extent, leisure—move in the opposite direction. A specular pattern is observed for men: their working time decreases as the wife's share approaches 0.5 and then jumps once she becomes the higher earner, with childcare exhibiting a corresponding break in slope. The discontinuity in leisure is clear for men but much less pronounced for women.[12]

[10] Observations implying hourly wages above 100 are dropped, as the variable is truncated.

[11] The wage-share variable is trimmed to the interval $(0.25, 0.75)$ to avoid sparse extreme observations.

[12] Leisure dynamics are more complex than work or childcare. On one hand, higher relative wages reduce leisure by increasing work hours; on the other, a higher Pareto weight raises the consumption of private goods, including leisure itself (Blundell et al. 2018).

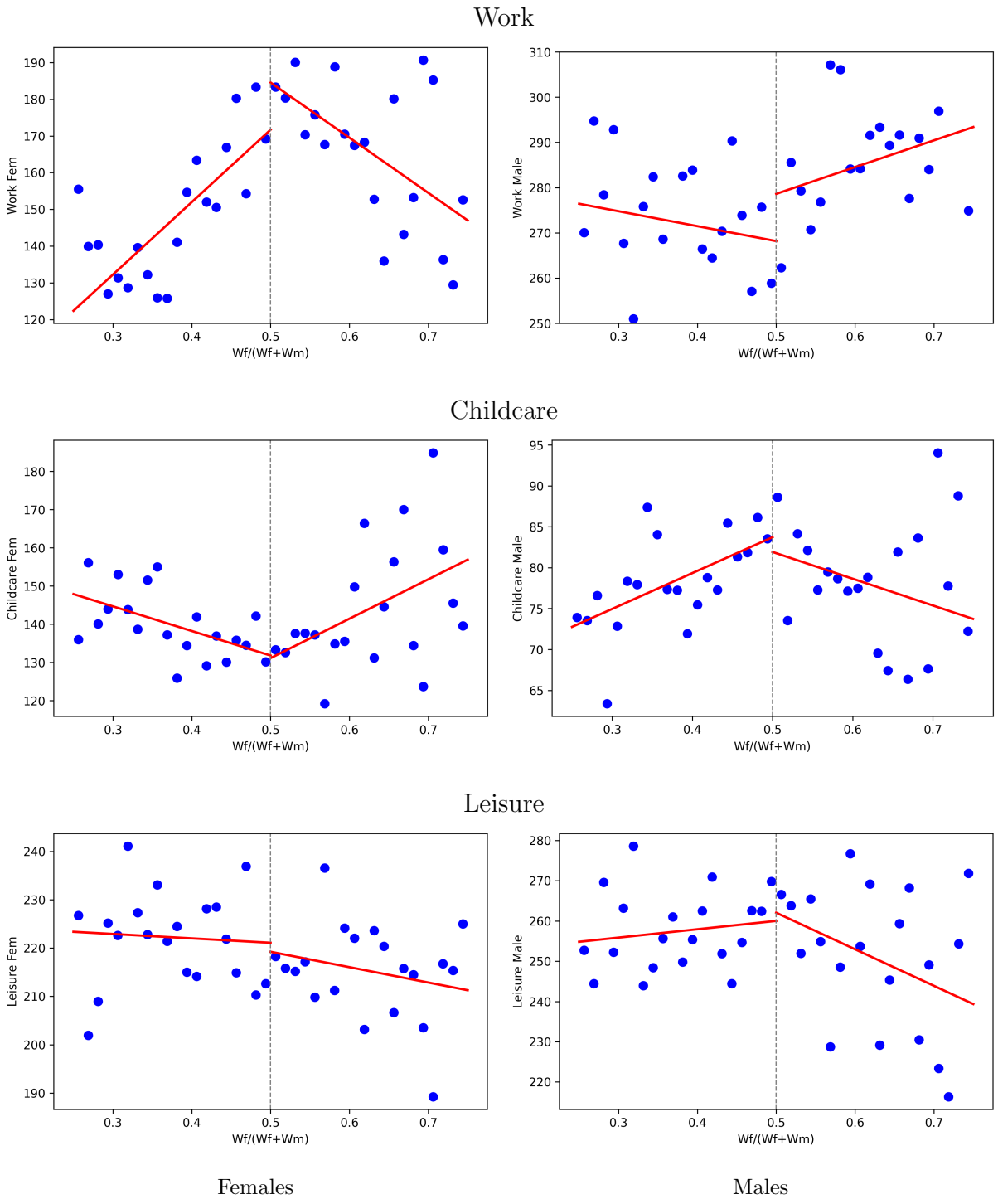

Figure 4: Relationship between a wife's wage share and average daily minutes devoted to work, childcare, and leisure.

4.2 Model set-up

The model is based on a semi-cooperative framework. This stems from the fact that the data show a kink at equal wages and frequent childcare corners (one parent does none on the diary day). A fully cooperative model tends to smooth these away unless ad–hoc frictions are added. A semi–cooperative setup instead treats market hours as contractible and jointly chosen, and childcare as a non–contractible, privately provided public good chosen non–cooperatively. Each spouse's childcare best response has a flat zero region (free-riding when the other invests enough) which lines up with the measurements and reproduces the kink and the corners with minimal extra structure.

A household consists of two members, $i \in \{f, m\}$, each characterized by a market wage rate w_i, caring for n children, and endowed with one unit of time. Family members engage in a two-stage game. In the first stage, they jointly determine their optimal market labor supply; in the second stage, each individually chooses the time allocated to childcare.

Time budget. Each individual faces the time constraint

$$h_i + l_i + (t_i + \tilde{t}_i)\, n \leq 1, \quad h_i > 0,\ l_i > 0,\ t_i > 0,\ \tilde{t}_i > 0, \tag{9}$$

where h_i denotes market work time, l_i leisure time, t_i parental time invested per child in human capital, $\tilde{t}_i$ the fixed (non-quality) childcare time cost per child, and n the number of children.

The quality of children is given by

$$q = (1 + t_f)^{\alpha}\,(1 + t_m)^{1-\alpha}, \tag{10}$$

with $\alpha \in [0, 1]$ governing the relative effectiveness of maternal versus paternal time inputs. Following Del Boca et al. (2013), consumption goods are assumed to have a negligible effect on child quality, so only time inputs enter this production function, which allows for corner solutions in optimal childcare supply.

Utility and identity norm. Individual i's baseline utility is

$$u_i \;=\; \log(c) \;+\; \mu_i \log(l_i) \;+\; \gamma_i \log(q\, n). \tag{11}$$

Following the social-norm tax frameworks of Greenwood et al. (2016)[13] and Doepke and

[13]They specify household resources as $c = (1 - \tau_t) w_f h_f + w_m h_m$, where τ_t is an exogenous, time-varying tax that captures gradually weakening anti-work norms against women; a decline in τ_t over time drives the

Kindermann (2019)[14], consumable income is adjusted by a norm-dependent tax on the wife's earnings:

$$c \;=\; \phi(s)\, w_f h_f \;+\; w_m h_m, \qquad s \;=\; \frac{w_f}{w_f + w_m}. \tag{12}$$

In this model, the backlash emerges as the wife's share of household income approaches that of her husband. Accordingly, the social-norm tax is specified as a nonlinear, endogenous function of the wife's relative income:

$$\phi(s) \;=\; \exp\!\big[-\chi\, s^{\kappa}\big], \quad \chi > 0,\ \kappa > 1.$$

Unlike previous formulations, the tax rate here depends non-linearly on s, ensuring that social costs only materialize once the wife's wage share crosses a threshold determined by χ and κ, while keeping consumption strictly positive.

Stages. Agents play a two-stage semi-cooperative game à la Cournot. The problem is solved by backward induction. In the second stage, each individual chooses the amount of childcare provision by maximizing the following objective function:

$$v_i = \log(c) \;+\; \mu_i \log\!\big(1 - h_i - (t_i + \tilde{t}_i)\, n\big) \;+\; \gamma_i \log\!\big((1+t_f)^{\alpha}(1+t_m)^{1-\alpha} n\big), \tag{13}$$

with h_i given from the first stage. There are four possible regimes: both, one, or neither spouse provides childcare.

Under mild regularity conditions the two-stage semi-cooperative game admits a unique subgame perfect equilibrium. In particular, since each spouse's time-allocation choice in stage 2 solves a strictly concave maximization over the compact, convex set

$$\{t_i \geq 0 :\; h_i + l_i + (t_i + \tilde{t}_i) n \leq 1\},$$

and the induced household payoff in stage 1, where the agents maximize the household utility function, given by the weighted sum of the individuals'

$$u_h \;=\; \theta\, u_m \;+\; (1-\theta)\, u_f,$$

where $\theta \in (0,1)$ denotes the bargaining power of the wife. Since the utility is continuous in (h_f, h_m) and diagonally strictly concave, Brouwer's fixed-point theorem ensures existence,

post-1960 rise in female labour supply.

[14]They model fertility bargaining by assigning the wife a constant cost share $\chi^f > 0$ of child-rearing expenditures, so her effective resources are $(1-\chi^f)w_f h_f$; a larger χ^f, interpreted as a stricter gender norm, reduces her outside option, acting like a multiplicative wedge on her earnings.

while Rosen (1965) diagonal strict concavity argument guarantees uniqueness of the profile $(h_f^*, h_m^*, t_f^*, t_m^*)$. Hence the model admits one equilibrium. Depending on the second-stage outcome, either both spouses work or only one does, yielding the twelve solution profiles reported in Appendix Section D.

Assumptions. **A1 (Primitives).** Preferences are as in (11) with $\mu_i > 0$, $\gamma_i > 0$, $\alpha \in (0,1)$, wages $w_i > 0$, number of children $n \in \mathbb{N}$, and fixed time costs $\tilde{t}_i \geq 0$ such that $1 - n\tilde{t}_i > 0$ for $i \in \{f, m\}$.
A2 (Norm wedge). $\phi : [0,1] \to (0,1]$ is C^2, strictly decreasing and log–convex in s (e.g. $\phi(s) = \exp[-\chi s^\kappa]$ with $\chi > 0$, $\kappa > 1$). When s is defined on *earnings* $s = \frac{w_f h_f}{w_f h_f + w_m h_m}$, the map $(h_f, h_m) \mapsto \log\big(\phi(s)\, w_f h_f + w_m h_m\big)$ is strictly concave on the feasible set.[15]
A3 (Feasible sets). For any (h_f, h_m) with $0 \leq h_i \leq 1 - n\tilde{t}_i$, each player's second–stage choice set for t_i is nonempty, convex, and compact; the joint feasible set for (h_f, h_m, t_f, t_m) is nonempty, convex, and compact.

Proposition 1 (Existence and uniqueness)**.** *Under A1–A3:*

(i) ***Stage 2 (childcare).*** *For any (h_f, h_m), the second–stage game in (t_f, t_m) is a diagonally strictly concave game; hence it admits a* unique *Nash equilibrium (t_f^*, t_m^*) (Rosen's theorem). The equilibrium correspondence $(t_f^*, t_m^*)(h_f, h_m)$ is single–valued and continuous.*

(ii) ***Stage 1 (market work).*** *Let*

$$V(h_f, h_m) = \theta\, v_f\big(h_f, h_m, t^*(h_f, h_m)\big) + (1-\theta)\, v_m\big(h_f, h_m, t^*(h_f, h_m)\big)$$

denote the household objective induced by the unique stage-2 equilibrium. Under A2, V is strictly concave on the feasible set of (h_f, h_m); therefore the stage-1 problem has a unique *maximizer (h_f^*, h_m^*).*

Consequently, the two–stage semi-cooperative problem has a unique *subgame-perfect equilibrium $(h_f^*, h_m^*, t_f^*, t_m^*)$.*

4.3 Estimation

The model is calibrated to replicate stylized facts about the relationship between women's market work, childcare time, and their share of household wages. Wages and the number of

[15] A sufficient condition (proved in Appendix D.1) is $\chi \leq \bar{\chi}(\kappa, w_f, w_m, \underline{h}, \overline{h})$ for bounds $0 < \underline{h} \leq h_i \leq \overline{h} < 1$ implied by the time constraint. If s is defined on *potential shares*, ϕ is independent of (h_f, h_m) and strict concavity is immediate.

children are drawn from log-normal distributions using summary statistics from the ATUS sample (Table 6).[16]

Table 6: Summary statistics

Variable	Mean	Std. Dev.
Female wages	16.309	9.366
Male wages	18.904	10.084
Number of children	2.105	0.978

The bargaining power parameter θ_i is assumed to follow a logistic-normal distribution:

$$\theta_i \;=\; \frac{1}{1+\exp(-z_i)}, \qquad z_i \;\sim\; \mathcal{N}\big(\bar{\theta},\, \sigma^2\big),$$

so that $\theta_i \in (0,1)$, and where $\bar{\theta}$ and σ^2 denote the mean and variance of the underlying normal distribution, respectively.

Preference for consumption is normalized to one. With log utility, only the ratios between the preference weights on consumption, leisure, and child quality are identified by time–use moments; scaling all utility weights by a constant leaves choices unchanged. Since we do not observe consumption quantities, fixing the consumption weight pins down the utility scale and avoids weak identification of levels. The child-quality productivity parameter, α, is set to 0.5, following Del Boca et al. (2013) and Gobbi (2018). The remaining parameters

$$(\gamma_f,\, \gamma_m,\, \mu_f,\, \mu_m,\, \tilde{t}_f,\, \tilde{t}_m,\, \bar{\theta},\, \sigma,\, \chi,\, \kappa)$$

are estimated via the Method of Simulated Moments. Specifically, we solve

$$\hat{p} = \arg\min_{p} \left(\tfrac{m-\hat{m}(p)}{m}\right)' I \left(\tfrac{m-\hat{m}(p)}{m}\right), \tag{14}$$

where m stacks mean market–work and childcare shares in five bins of the wife's wage share $\frac{w_f}{w_f+w_m} \in (0.25, 0.75)$ (20 moments total). The identity weighting matrix I is used for three reasons: (i) the targeted moments are already scale–standardized (squared percentage gaps), so equal weighting is close to efficient; (ii) ATUS diary measures are zero–inflated and heteroskedastic with thin bins, making the sample moment covariance noisy and potentially ill–conditioned; and (iii) The minimization proceeds in two stages: a Differential Evolution search provides a candidate minimum, which seeds a local quadratic–approximation routine. $W = I$ yields a smoother, well–conditioned objective that improves stability for a global–plus–local optimizer.

[16] Nominal wages are deflated to constant-2000 dollars.

Table 7 presents the parameter estimated by simulating 50,000 households, both with and without the family social norm. The coefficients on childcare quality exceed those on leisure, with the quality weight for women being slightly lower. By contrast, the fixed childcare share is higher for women (0.09) than for men (0.05). The logistic-normal specification for bargaining power implies an average female Pareto weight of approximately 0.43. Estimating the model without the norm does not substantially alter the parameters' orders of magnitude: fixed childcare costs remain higher for women and vice-versa for the weight on quality care, while the variable childcare time and leisure preference parameters stay slightly above one.

Table 7: Estimates for the parameters

Parameters	Description	Estimates	
		$\phi \neq 1$	$\phi = 1$
γ_f, γ_m	Preferences for child quality	3.67, 4.48	1.49, 4.02
$\tilde{t}_f, \tilde{t}_m$	Share of fixed childcare	0.09, 0.05	0.08, 0.06
μ_f, μ_m	Preferences for leisure	1.19, 1.11	1.15, 1.37
$\bar{\theta}, \sigma$	Moments of bargaining power distrib.	-0.45, 1.98	0.35, 1.75
κ, χ_f	Female labor-supply distortion	4.19, 7.27	

4.4 Numerical results

Using the estimated parameters, this section first compares the simulated moments with those used for estimation. It then presents counterfactual analyses showing how households respond to wage shocks at different points in the income distribution.

4.4.1 Comparison with data

Table 8 compares empirical averages for time spent working, childcare, and employment rates with those generated by the model using the parameters in Table 7. The model reproduces the observed averages closely: men allocate approximately half of their time budget to market work and 13% to childcare, while women allocate about one quarter to market work and 23% to childcare. Employment rates—excluded from the SMM objective—also align reasonably well: the model predicts nearly 100% male employment (similarly to the data) and 57% female employment (versus 68% in the data).

Figure 5 shows the simulated values for working and childcaring time, for different bins in the relative wages of women. The values exhibit a change in direction around the wage equalization point, with ranges that are fairly close to those observed in the ATUS sample.

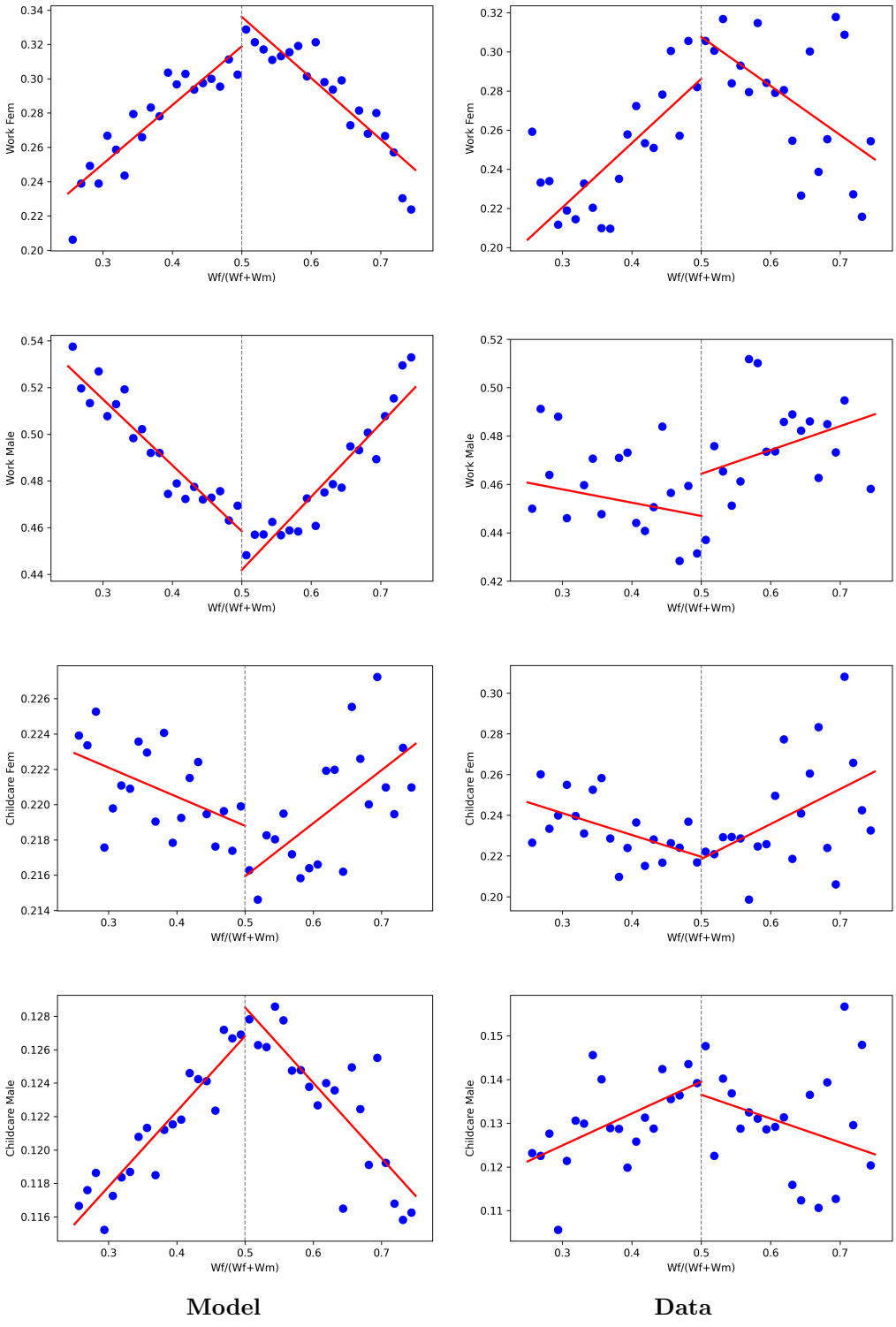

Figure 5: Simulated and data work and childcare time shares.

Table 8: Comparison of model and data averages

Sex	Moment	Model mean ($\phi \neq 1$)	Model mean ($\phi = 1$)	Data mean
Internal moments				
Male	Work	0.4989	0.4360	0.4709
	Childcare	0.1207	0.1303	0.1280
Female	Work	0.2608	0.3006	0.2443
	Childcare	0.2210	0.1755	0.2342
External moments				
Male	Employment	0.9999	0.8543	0.9715
Female	Employment	0.5663	0.7163	0.6775

4.4.2 Counterfactuals

Empirical studies of both the U.S. robot wave and the China import shock show that the observed narrowing of the gender wage gap is driven primarily by declining earnings—or outright job loss—among men in the bottom-to-middle terciles, whereas compression on the female side arises from modest gains concentrated in the upper terciles of women's distribution (see, e.g., Acemoglu and Restrepo, 2020; Autor et al., 2013; Cortes et al., 2024).

To replicate this pattern quantitatively, simulations impose wage shocks on different terciles of the male and female wage distributions. Figure 6 plots the resulting differences in time use between spouses—namely, men's work time minus women's work time, and women's childcare time minus men's childcare time—under both the baseline model (including the social norm $\phi(w_f, w_m)$) and the counterfactual without the norm, as well as their difference.

A strong increase in women's potential wages in the top tercile leads to a rise in the work-time differential: a 1% increase in the differential when women's market wages increase by half. Conversely, reductions in men's wages in the bottom tercile produce a more pronounced effect, yielding a 2% increase in the differential when men's wages are halved. These shocks also induce moderate changes in the childcare-time differential.

Relative to the no-norm counterfactual, the presence of the social norm amplifies these differentials by just over 10% for work time and about 5% for childcare time. Moreover, the gap between the two simulations widens as wage variations are applied across all three terciles of the distribution.

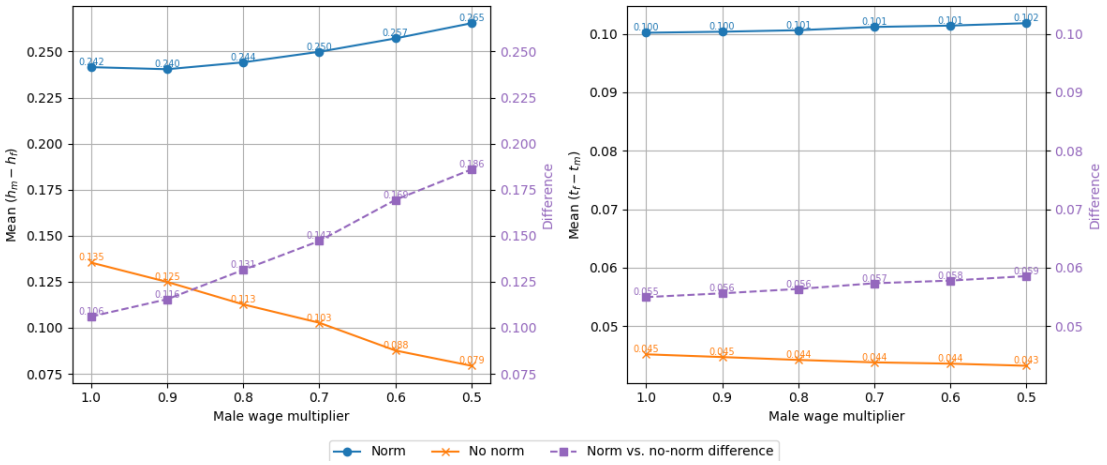

Negative shock to men's wages in the first tercile

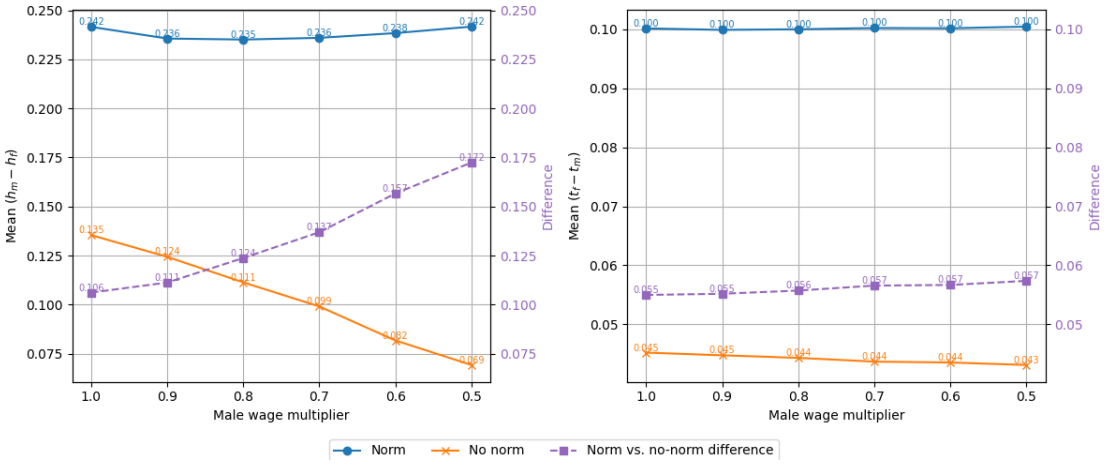

Negative shock to men's wages in the second tercile

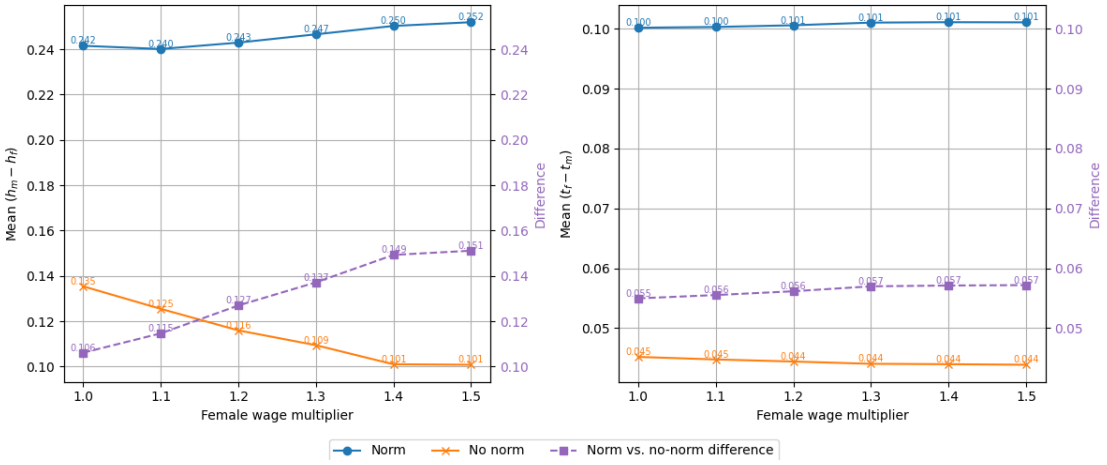

Positive shock to women's wages in the third tercile

Figure 6: Simulated time use divergence in relation to market wage variations at different terciles.

The calibrated semi-cooperative model formalises the causal intuition for the results presented in Section 3. A negative shock to men's wages raises the wife's wage share and, through the identity cost embedded in the consumption aggregator, creates an endogenous threshold $s^\star$ around equal earnings. Below $s^\star$, standard labor-supply forces dominate and women's market hours rise with their relative wage; above $s^\star$, the identity cost reduces the marginal payoff to additional female market hours, flipping the slope and shifting time into childcare and leisure, with mirror responses for men. Because the size of the wage-share shift is greatest near or above parity, aggregate effects scale nonlinearly with the cross-household distribution of relative wages: counterfactuals show that (i) declines in men's wages in the lower terciles move more couples past $s^\star$ than equivalent gains at the top of the women's distribution, and (ii) the share of couples for which the norm binds increases when shocks compress the gender wage gap, amplifying gaps in time use. In short, the model reproduces the kink at parity, the inverse-U in women's market hours (and the mirror in childcare), and the distributional scaling of these effects documented in the data.

5 Conclusion

This paper examines how two pervasive forces in modern labor markets—industrial automation and import competition—reshape the allocation of time within households. Linking ATUS time diaries to commuting-zone exposure to robots and the China shock, and addressing endogeneity with external industry shifters, I find systematic within-couple reallocations. Greater exposure to robots leads women to shift time out of market work and into childcare and leisure, while men increase market work and reduce leisure. Quantitatively, one additional robot per 1,000 workers reallocates roughly one hour per week at the household level across work, childcare, and leisure. Exposure to Chinese import penetration similarly pushes couples toward the non-market margin for women: an extra $1,000 of imports per worker lowers women's market hours by about three hours per week.

These empirical patterns are rationalized by a structural household model featuring an identity norm that penalizes couples when the wife out-earns the husband. The model reproduces the observed non-linearities in time use: as the wife's potential wage share rises toward parity, her market hours increase, but once the breadwinner threshold is crossed, the identity cost triggers a withdrawal from the labor market and a sharp increase in childcare time. Counterfactual simulations indicate that this norm roughly doubles the gender gap in market hours relative to an identity-neutral benchmark. Crucially, because automation and trade shocks disproportionately depress men's wages in the lower-middle distribution, they push a significant mass of couples into the region where this norm binds, amplifying gender

gaps in time use even as the wage gap narrows.

The findings highlight that cultural norms can act as a friction preventing the efficient allocation of time following economic shocks. This suggests several avenues for policy intervention.

First, policies that subsidize substitutes for home production can weaken the identity mechanism. Since the norm manifests primarily through the substitution of female market work for childcare, policies that lower the cost of childcare and early education are particularly relevant. If high-quality external care is affordable and accessible, the relative price of specializing in home production rises, potentially offsetting the identity tax that discourages women from working when their husbands' earnings fall.

Second, the results provide a novel argument for targeted wage insurance. Standard trade adjustment assistance often focuses on retraining displaced workers. However, this paper shows that a drop in the husband's wage can trigger a secondary withdrawal of the wife from the labor force. Wage insurance schemes that shore up the earnings of displaced male workers could, counter-intuitively, prevent the decline of female labor supply by keeping households away from the identity discontinuity where the breadwinner norm binds.

Third, place-based policies must account for the gendered nature of local demand shocks. Regional development policies often aim to restore manufacturing jobs. However, given the structural shift toward services—where women often hold a comparative advantage—development strategies should also facilitate the transition of men into service-sector roles. Reducing the strong gender segregation of occupations would align labor demand with household supply and, over the long term, potentially soften the rigidity of identity norms.

In sum, automation and trade do not only reallocate tasks across firms; they reallocate time within households. When relative wages move couples toward earnings parity, social norms can paradoxically reverse progress in gender equality. Recognizing and quantifying this interaction is essential for designing policies that ensure the benefits of technological change are distributed efficiently within the family.

References

Acemoglu, D. and Restrepo, P. (2020). Robots and jobs: Evidence from us labor markets. *Journal of Political Economy*, 128(6):2188–2244.

Adão, R., Kolesár, M., and Morales, E. (2019). Shift-share designs: Theory and inference*. *The Quarterly Journal of Economics*, 134(4):1949–2010.

Anelli, M., Giuntella, O., and Stella, L. (2021). Robots, marriageable men, family, and fertility. *Journal of Human Resources*, page 1020.

Autor, D., Dorn, D., and Hanson, G. (2019). When work disappears: Manufacturing decline and the falling marriage market value of young men. *American Economic Review: Insights*, 1(2):161–78.

Autor, D. H. and Dorn, D. (2013). The growth of low-skill service jobs and the polarization of the us labor market. *American Economic Review*, 103(5):1553–97.

Autor, D. H., Dorn, D., and Hanson, G. H. (2013). The china syndrome: Local labor market effects of import competition in the united states. *American Economic Review*, 103(6):2121–68.

Becker, G. S. (1965). A theory of the allocation of time. *The Economic Journal*, 75(299):493–517.

Bertrand, M., Kamenica, E., and Pan, J. (2015). Gender identity and relative income within households. *The Quarterly Journal of Economics*, 130(2):571–614.

Besedeš, T., Lee, S. H., and Yang, T. (2021). Trade liberalization and gender gaps in local labor market outcomes: Dimensions of adjustment in the united states. *Journal of Economic Behavior & Organization*, 183:574–588.

Blundell, R., Pistaferri, L., and Saporta-Eksten, I. (2018). Children, Time Allocation, and Consumption Insurance. *Journal of Political Economy*, 126(S1):73–115.

Bursztyn, L., Fujiwara, T., and Pallais, A. (2017). 'acting wife': Marriage market incentives and labor market investments. *American Economic Review*, 107(11):3288–3319.

Chiappori, P.-A. (1992). Collective labor supply and welfare. *Journal of Political Economy*, 100(3):437–467.

Cortes, P., Feng, Y., Guida-Johnson, N., and Pan, J. (2024). Automation and gender: Implications for occupational segregation and the gender skill gap. NBER Working Paper 32030, National Bureau of Economic Research.

Costanzo, C. (2025). Robots, jobs, and optimal fertility timing. *Journal of Population Economics*, 38(2):1–33.

de Vries, G. J., Gentile, E., Miroudot, S., and Wacker, K. M. (2020). The rise of robots and the fall of routine jobs. *Labour Economics*, 66:101885.

Del Boca, D., Flinn, C., and Wiswall, M. (2013). Household Choices and Child Development. *The Review of Economic Studies*, 81(1):137–185.

Doepke, M. and Kindermann, F. (2019). Bargaining over babies: Theory, evidence, and policy implications. *American Economic Review*, 109(9):3264–3306.

Flood, S., King, M., Rodgers, R., Ruggles, S., Warren, J. R., Backman, D., Chen, A., Cooper, G., Richards, S., Schouweiler, M., and Westberry, M. (2024). IPUMS CPS: Version 12.0 [dataset]. Minneapolis, MN: IPUMS.

Folke, O. and Rickne, J. (2020). All the single ladies: Job promotions and the durability of marriage. *American Economic Journal: Applied Economics*, 12(1):260–287.

Ge, S. and Zhou, Y. (2020). Robots, computers, and the gender wage gap. *Journal of Economic Behavior & Organization*, 178:194–222.

Getik, D. (2024). Relative Income and Mental Health in Couples. *The Economic Journal*, page 3291–3305.

Gobbi, P. E. (2018). Childcare and commitment within households. *Journal of Economic Theory*, 176:503–551.

Goldsmith-Pinkham, P., Sorkin, I., and Swift, H. (2020). Bartik instruments: What, when, why, and how. *American Economic Review*, 110(8):2586–2624.

Greenwood, J., Guner, N., Kocharkov, G., and Santos, C. (2016). Technology and the changing family: A unified model of marriage, divorce, educational attainment, and female labor-force participation. *The Review of Economic Studies*, 83(1):157–199.

Gronau, R. (1977). Leisure, home production, and work—the theory of the allocation of time revisited. *Journal of Political Economy*, 85(6):1099–1123.

Hamermesh, D. S., Frazis, H., and Stewart, J. (2005). Data watch: The american time use survey. *Journal of Economic Perspectives*, 19(1):221–232.

Heggeness, M. and Murray-Close, M. (2019). Manning up and womaning down: How husbands and wives report earnings when she earns more. Opportunity and Inclusive Growth Institute Working Papers 28, Federal Reserve Bank of Minneapolis.

ISSP Research Group (2016). International social survey programme: Family and changing gender roles iv - issp 2012. GESIS Datenarchiv, Köln. Available online at https://doi.org/10.4232/1.12661.

Keller, W. and Utar, H. (2022). Globalization, gender, and the family. *The Review of Economic Studies*, 89(6):3381–3409.

Kleibergen, F. and Paap, R. (2006). Generalized reduced rank tests using the singular value decomposition. *Journal of Econometrics*, 133(1):97–126.

Rosen, J. B. (1965). Existence and uniqueness of equilibrium points for concave n-person games. *Econometrica*, 33(3):520–534.

Rosenberg, S. (2021). Revisiting the Breadwinner Norm: The effect of potential relative earnings on married women's labor supply. Manuscript, ECARES, Université Libre de Bruxelles.

Stewart, J. (2013). Tobit or not tobit? *Journal of Economic and Social Measurement*, 38(3):263–290.

van Ark, B. and Jäger, K. (2017). Recent trends in europe's output and productivity growth performance at the sector level, 2002-2015. *International Productivity Monitor*, 33:8–23.

Webb, M. (2019). The Impact of Artificial Intelligence on the Labor Market.

Zinovyeva, N. and Tverdostup, M. (2021). Gender identity, coworking spouses, and relative income within households. *American Economic Journal: Applied Economics*, 13(4):258–84.

Acknowledgements

Funding This project has been funded by the Belgian National Fund for Scientific Research (FNRS).

Data availability The following data sources have been used for the analysis in this article:

- **American Time Use Survey (ATUS)** – U.S. Bureau of Labor Statistics, 2003–2023.
- **Current Population Survey (CPS)** – ASEC and basic monthly files, via IPUMS-CPS (Flood et al. 2024 release); 1990–2023.
- **ISSP "Family and Changing Gender Roles IV"** – 2012 U.S. subsample.
- Patent-based automation-risk scores – Webb (2020, *American Economic Review: Insights* 2(3): 300-17).
- O*NET manual-task intensity scores – Autor & Dorn (2013, *AER* 103(5): 1553-97).
- 1990 commuting-zone × industry employment shares – Acemoglu & Restrepo (2020, *JPE* 128(6): 2188-2244).
- 1970 commuting-zone × industry employment shares – Decennial IPUMS data.
- Industrial-robot stocks (country × industry, 1993-2019) – International Federation of Robotics, *World Robotics* database.
- 1990 industry employment for EU-5 (used in the robot instrument) – EU KLEMS Growth & Productivity Accounts, 2017 edition.
- U.S. import-exposure, domestic absorption and baseline instrument files – Autor, Dorn & Hanson (2013, "The China Syndrome," *AER* 103(6): 2121-68).
- Chinese exports to eight alternative OECD markets (trade instrument) – UN Comtrade extraction following Autor–Dorn–Hanson.
- Commuting-zone boundaries and county cross-walks – Autor, Dorn & Hanson replication materials (2013).

Declarations

Conflict of interest The author declares that he has no conflict of interest.

Appendix

A Supplementary tables

Table A1: Descriptive statistics: ATUS general population

	Females			Males		
Variable	Obs	Mean	Std. Dev.	Obs	Mean	Std. Dev.
Leisure (min/day)	122,710	310.07	208.33	96,658	356.87	235.57
Childcare (min/day)	122,710	43.10	101.62	96,658	22.34	69.34
Market work (min/day)	122,710	126.61	217.06	96,658	191.39	261.12
Age	122,710	48.37	18.15	96,658	46.77	17.44
Hourly wage (USD)	35,769	15.08	9.23	29,080	17.52	10.25
Weekly earnings (USD)	61,698	709.03	513.95	54,518	951.10	596.42
Usual work hours per week	113,670	21.20	20.66	88,373	30.94	22.49
Less than secondary (%)	122,710	14.37	35.08	96,658	15.69	36.37
Secondary (%)	122,710	25.91	43.81	96,658	25.52	43.60
Some college (%)	122,710	27.95	44.87	96,658	25.39	43.52
Tertiary (%)	122,710	31.77	46.56	96,658	33.40	47.17

Notes: "General population" includes all ATUS respondents by sex. Variable definitions as in Table 1.

Table A2: Effect of Robot exposure on wages and wage gap (3 and 10-year differences).

	3-Year Differences			**10-Year Differences**		
	(1)	(2)	(3)	(4)	(5)	(6)
	Male Wages	Female Wages	Wage Gap	Male Wages	Female Wages	Wage Gap
Robot	0.008	-0.003	0.015*	-0.002	-0.000	-0.000
	(0.007)	(0.006)	(0.009)	(0.006)	(0.007)	(0.007)
$\text{Robot}^{\text{2SLS}}$	-0.056***	-0.011	-0.036*	-0.002	0.008	-0.009
	(0.018)	(0.019)	(0.020)	(0.007)	(0.009)	(0.012)
Observations	1,233	1,270	1,158	512	527	477
R^2 (OLS)	0.038	0.016	0.035	0.038	0.028	0.041

Sample: Working age individuals (18-64) in the ATUS. The dependent variable is the long difference (3 or 10 years) of the log hourly wage for men, women, or the gender gap. "Robot" variables represent the change in exposure to robotization (EXP). All specifications include 1990 baseline controls (demographics and industry shares) and year fixed effects. Robust standard errors clustered at the commuting-zone level are in parentheses. *** $p < 0.01$, ** $p < 0.05$, * $p < 0.1$.

Table A3: Effect of China shock on wages and wage gap (3 and 10-year differences).

	3-Year Differences			**10-Year Differences**		
	(1)	(2)	(3)	(4)	(5)	(6)
	Male Wages	Female Wages	Wage Gap	Male Wages	Female Wages	Wage Gap
Trade_{Male}	8.678	-4.094	14.92	2.263	14.68	-13.50
	(13.33)	(7.33)	(16.60)	(13.08)	(22.58)	(22.51)
$\text{Trade}_{Male}^{\text{2SLS}}$	53.83	30.20	29.06	2.757	33.93	-26.49
	(50.15)	(46.05)	(52.46)	(20.89)	(23.34)	(24.36)
Trade_{Fem}	-12.28	3.578	-19.73	-8.872	-54.96*	50.21
	(19.56)	(11.71)	(25.61)	(25.02)	(30.47)	(33.33)
$\text{Trade}_{Fem}^{\text{2SLS}}$	-68.77	-37.99	-38.65	-2.047	-72.12**	65.73*
	(65.51)	(62.66)	(73.22)	(33.70)	(36.85)	(38.31)
Observations	1,045	1,085	993	185	181	176
R^2 (OLS)	0.042	0.014	0.031	0.068	0.162	0.086

Sample: Working age individuals (18-64) in the ATUS. The dependent variable is the long difference (3 or 10 years) of the log hourly wage for men, women, or the gender gap. "Trade" variables represent the change in import exposure per worker. All specifications include 1990 baseline controls (demographics and industry shares) and year fixed effects. Robust standard errors clustered at the commuting-zone level are in parentheses. *** $p < 0.01$, ** $p < 0.05$, * $p < 0.1$.

Table A4: Effect of robots on time spent working, childcaring, and leisuring per day. Sample: respondents with no spouse or unmarried partner.

	Males		Females	
	Work	Leisure	Work	Leisure
Robots				
Robots	-1.270	6.134	4.075	-4.857
	(4.630)	(3.839)	(3.360)	(3.014)
$\text{Robots}^{\text{2SLS}}$	-1.030	5.324	7.234	-7.132*
	(6.457)	(5.137)	(4.652)	(4.314)
Observations	8,519	8,519	11,741	11,741
R-squared	0.318	0.246	0.312	0.187
China shock				
Trade	424.3	-296.8	81.76	-1,490**
	(1,398)	(971.6)	(1,396)	(742.9)
$\text{Trade}^{\text{2SLS}}$	-1,404	718.9	-2.348	-1,611
	(1,617)	(1,306)	(1,580)	(1,249)
Observations	7,318	7,318	10,232	10,232
R-squared	0.300	0.239	0.295	0.166
Decomposed China shock				
Trade_{Male}	4,181	-3,805	420.2	-2,998
	(5,644)	(3,278)	(3,408)	(2,371)
Trade_{Fem}	-6,132	5,835	-89.34	1,103
	(7,856)	(5,714)	(5,447)	(3,780)
$\text{Trade}^{\text{2SLS}}_{Male}$	1,887	-10,374	4,184	-8,150
	(8,705)	(7,294)	(7,052)	(8,349)
$\text{Trade}^{\text{2SLS}}_{Fem}$	-6,944	18,662*	-6,363	8,668
	(13,263)	(11,239)	(10,135)	(11,320)
Observations	7,318	7,318	10,232	10,232
R-squared	0.300	0.240	0.296	0.166
Respondent employed	✓	✓	✓	✓

Controls include state×year FE, respondent's age/education, day, month, holiday. SEs clustered at CZ×year. *** $p < 0.01$, ** $p < 0.05$, * $p < 0.1$.

Table A5: Effect of robot and trade shock on hours worked per week.

	Males			Females		
Weekly hours worked	(1)	(2)	(3)	(4)	(5)	(6)
Robots						
Robots	-0.0355	-0.189	-0.0340	-0.722**	-1.070***	-0.872***
	(0.221)	(0.140)	(0.222)	(0.342)	(0.276)	(0.288)
$\text{Robots}^{\text{2SLS}}$	-0.168	-0.0430	-0.159	-1.010**	-1.345***	-1.026**
	(0.316)	(0.203)	(0.286)	(0.464)	(0.390)	(0.421)
China shock						
Trade	-173.3	-57.03	-109.6	145.1	-193.0*	-237.1**
	(112.6)	(67.36)	(81.76)	(105.7)	(100.8)	(100.4)
$\text{Trade}^{\text{2SLS}}$	-33.14	-72.17	-44.72	89.82	-182.7**	-234.4***
	(73.58)	(50.73)	(65.94)	(99.10)	(86.06)	(84.99)
Decomposed China shock						
Trade_{Male}	718.0**	64.80	664.0***	320.8	17.70	-40.96
	(306.4)	(167.7)	(249.7)	(269.1)	(209.3)	(220.2)
Trade_{Fem}	-1,258**	-303.0	-1,196***	-301.9	-513.0	-558.4
	(504.4)	(303.3)	(439.8)	(424.3)	(381.7)	(416.8)
$\text{Trade}^{\text{2SLS}}_{Male}$	607.7	326.8	699.4*	809.8*	190.9	242.7
	(497.7)	(274.3)	(371.3)	(473.9)	(388.9)	(423.2)
$\text{Trade}^{\text{2SLS}}_{Fem}$	-1,350*	-637.9	-1,325**	-933.1	-787.4	-995.7
	(792.2)	(479.0)	(596.3)	(708.5)	(604.8)	(668.4)
Spouse employed	✓		✓	✓		✓
Respondent employed		✓	✓		✓	✓

Controls include state×year FE, spouse age/education, number of children (incl. under 5), children's age range, family income class, day, month, holiday. Sample: Individuals living with a spouse and children aged 10 or less. SEs clustered at CZ×year. *** $p < 0.01$, ** $p < 0.05$, * $p < 0.1$.

Table A6: Rotemberg Weights by Industry

Industry	Weight	Industry	Weight
Services	1.96e-10	Furniture	0.0099169
Metal Machinery	0.0084876	Vehicles Other	0.0130258
Agriculture	0.0084876	Mineral	0.0172633
Manufacturing, other	0.0084876	Metal Prod	0.0193203
Metal Products	0.0084876	Machinery	0.0229153
Construction	0.0086587	Food	0.0385796
Agriculture	0.0087799	Petrochemicals	0.0475847
Mining	0.0088249	Metal Basic	0.0813695
Research	0.0090184	Electronics	0.0836088
Textiles	0.0091325	Manufact Other	0.1217105
Utilities	0.0093328	Automotive	0.4475678
Paper	0.0094399		

Table A7: Effect of robots, with exposure net of the automotive industry, on time spent working, childcaring, and leisuring per day.

	Males			Females		
	(1)	(2)	(3)	(4)	(5)	(6)
Daily minutes work						
Robots	26.62*	3.766	37.65**	2.119	-8.446	-13.14
	(15.78)	(13.84)	(15.88)	(12.78)	(13.87)	(14.57)
$\text{Robots}^{\text{2SLS}}$	40.87	36.65	63.55	-29.01	-47.33	-39.74
	(42.46)	(43.88)	(43.38)	(31.08)	(34.93)	(36.65)
Daily minutes childcare						
Robots	-14.40**	0.785	-14.06*	8.914	10.39	16.47
	(7.304)	(7.140)	(7.644)	(10.61)	(10.53)	(13.91)
$\text{Robots}^{\text{2SLS}}$	-29.79*	3.174	-40.76**	34.96	29.66	29.90
	(17.54)	(21.28)	(18.61)	(25.47)	(24.42)	(30.14)
Daily minutes leisure						
Robots	-38.20***	-17.48*	-38.14***	6.446	3.732	8.911*
	(11.98)	(9.644)	(12.49)	(8.195)	(7.618)	(9.443)
$\text{Robots}^{\text{2SLS}}$	-0.0818	2.521	-20.64	14.81	23.07	40.73*
	(27.91)	(29.26)	(27.31)	(18.79)	(18.92)	(22.10)
Spouse employed	✓		✓	✓		✓
Respondent employed		✓	✓		✓	✓

Controls include state×year FE, spouse age/education, number of children (incl. under 5), children's age range, family income class, day, month, holiday. Sample: Individuals living with a spouse and children aged 10 or less. SEs clustered at CZ×year. *** $p < 0.01$, ** $p < 0.05$, * $p < 0.1$.

Table A8: Effect of robots on time spent working, childcaring, and leisuring per day, adjusting for commuting-zone-specific trends across quartiles of employment share in the automotive sector.

	Males			Females		
	(1)	(2)	(3)	(4)	(5)	(6)
Daily minutes work						
Robots	13.26***	8.315**	14.04**	-8.584**	-12.22**	-9.007*
	(5.097)	(3.313)	(6.078)	(4.054)	(4.850)	(5.274)
Robots^{2SLS}	14.44**	10.29**	16.99**	-11.32**	-13.49**	-10.65
	(6.968)	(4.514)	(7.935)	(5.224)	(6.300)	(6.768)
Daily minutes childcare						
Robots	1.675	1.172	2.077	2.102	5.555**	5.864**
	(1.727)	(1.338)	(1.807)	(2.214)	(2.277)	(2.758)
Robots^{2SLS}	1.913	2.307	1.212	3.918	9.218***	9.417***
	(2.503)	(1.976)	(2.645)	(3.094)	(2.873)	(3.644)
Daily minutes leisure						
Robots	-8.512***	-3.907	-9.641***	7.299***	9.962***	8.305***
	(2.759)	(2.801)	(3.591)	(2.467)	(2.675)	(3.060)
Robots^{2SLS}	-9.457***	-5.544*	-12.87***	7.294**	9.601***	9.024**
	(3.413)	(3.277)	(3.969)	(3.565)	(3.524)	(4.149)
Spouse employed	✓		✓	✓		✓
Respondent employed		✓	✓		✓	✓

Controls include state×year FE, spouse age/education, number of children (incl. under 5), children's age range, family income class, day, month, holiday. Sample: Individuals living with a spouse and children aged 10 or less. SEs clustered at CZ×year. *** $p < 0.01$, ** $p < 0.05$, * $p < 0.1$.

Table A9: Effect of robots on time spent working, childcaring, and leisuring per day. Adão et al. (2019) test for standard errors.

	Males			Females		
	(1)	(2)	(3)	(4)	(5)	(6)
Daily minutes work						
Robots	14.06***	6.63*	13.93***	-9.73*	-13.05***	-12.08***
	(0.89)	(3.56)	(0.42)	(5.10)	(2.34)	(3.28)
Robots^{2SLS}	13.92	8.38	18.02***	-15.40***	-18.91***	-15.26***
	(18.82)	(22.65)	(3.21)	(5.44)	(1.87)	(4.49)
Daily minutes childcare						
Robots	-0.49	0.70**	-0.41	1.99	4.62**	4.91***
	(0.76)	(0.36)	(1.16)	(4.65)	(2.14)	(1.72)
Robots^{2SLS}	0.16	1.69	-0.77	6.61	8.22	8.45***
	(1.30)	(15.66)	(6.88)	(5.27)	(6.12)	(1.43)
Daily minutes leisure						
Robots	-9.43***	-3.65***	-9.91***	7.09**	9.14**	8.89**
	(0.91)	(1.27)	(1.00)	(3.47)	(4.11)	(3.62)
Robots^{2SLS}	-8.79	-3.87	-11.87	6.75***	10.13***	9.41***
	(17.21)	(9.70)	(7.89)	(1.89)	(0.48)	(0.99)
Spouse employed	✓		✓	✓		✓
Respondent employed		✓	✓		✓	✓

Controls include state×year FE, spouse age/education, number of children (incl. under 5), children's age range, family income class, day, month, holiday. Sample: Individuals living with a spouse and children aged 10 or less. SEs clustered at CZ×year. *** $p < 0.01$, ** $p < 0.05$, * $p < 0.1$.

Table A10: Effect of trade shock on time spent working, childcaring, and leisuring per day. Adão et al. (2019) test for standard errors.

	Males			Females		
	(1)	(2)	(3)	(4)	(5)	(6)
Daily minutes work						
Trade_{Male}	11834.03***	7191.37***	12395.89***	3714.85**	1100.47***	-930.76***
	(846.46)	(398.87)	(1315.58)	(1648.58)	(27.16)	(120.72)
Trade_{Fem}	-30001.94***	-21226.07***	-30240.78***	-3600.64	-9161.62***	-7904.86***
	(1043.44)	(581.50)	(1759.87)	(2341.59)	(51.54)	(226.24)
$\text{Trade}^{\text{2SLS}}_{Male}$	12103.87***	3581.22***	8834.44***	3026.82***	-1077.93***	-4277.59***
	(737.76)	(286.58)	(996.64)	(819.53)	(53.03)	(47.24)
$\text{Trade}^{\text{2SLS}}_{Fem}$	-34282.03***	-20546.21***	-27757.79***	-476.73	-4555.91***	-1475.08***
	(863.96)	(217.17)	(1323.30)	(1331.99)	(37.70)	(80.52)
Daily minutes childcare						
Trade_{Male}	100.02	1269.73***	148.11	1050.38	1695.18***	1319.85***
	(624.05)	(139.28)	(768.43)	(1104.46)	(342.40)	(484.47)
Trade_{Fem}	2025.60**	174.59***	1517.54	-2470.68	987.82***	2669.73***
	(801.75)	(2.76)	(1034.06)	(1509.15)	(352.91)	(448.49)
$\text{Trade}^{\text{2SLS}}_{Male}$	6227.80***	4300.34***	6249.09***	-4137.86***	-1602.89***	-3066.27***
	(403.65)	(7.17)	(486.18)	(576.21)	(275.52)	(323.10)
$\text{Trade}^{\text{2SLS}}_{Fem}$	-6492.01***	-1308.75**	-7128.48***	5139.55***	5078.61***	8927.54***
	(463.67)	(539.79)	(603.02)	(843.79)	(317.67)	(258.93)
Daily minutes leisure						
Trade_{Male}	-17277.88***	-6120.81***	-17629.25***	-4088.89***	-1090.27***	-1632.79***
	(1278.91)	(72.30)	(1221.32)	(752.45)	(240.88)	(197.01)
Trade_{Fem}	24825.47***	10478.77***	25587.85***	4590.21***	1678.92***	3200.83***
	(1469.43)	(135.92)	(1573.75)	(1045.45)	(260.38)	(193.99)
$\text{Trade}^{\text{2SLS}}_{Male}$	-17611.39***	-5882.89***	-14710.59***	-809.26**	2043.17***	426.15***
	(1002.36)	(11.86)	(876.70)	(352.92)	(155.61)	(122.67)
$\text{Trade}^{\text{2SLS}}_{Fem}$	25301.63***	10115.26***	21617.73***	-2450.91***	-5011.65***	-1887.51***
	(1278.20)	(41.19)	(1280.18)	(538.33)	(141.53)	(82.25)
Spouse employed	✓		✓	✓		✓
Respondent employed		✓	✓		✓	✓

Controls include state×year FE, spouse age/education, number of children (incl. under 5), children's age range, family income class, day, month, holiday. Sample: Individuals living with a spouse and children aged 10 or less. SEs clustered at CZ×year. *** $p < 0.01$, ** $p < 0.05$, * $p < 0.1$.

B Supplementary figures

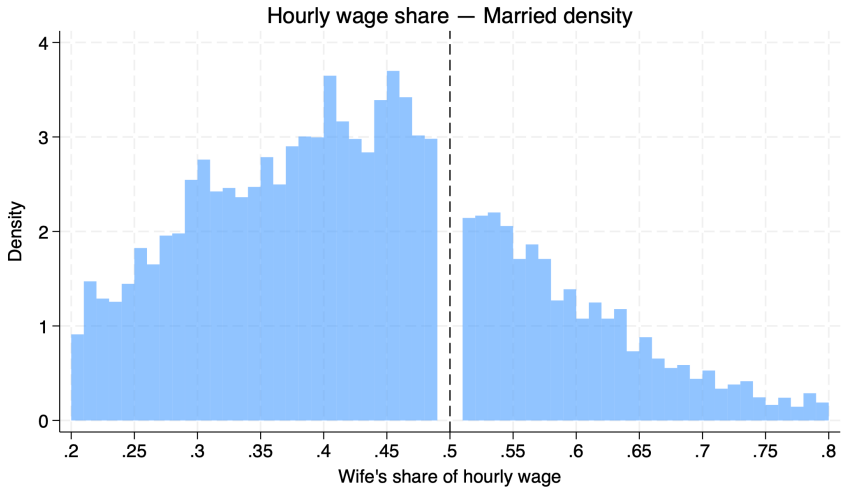

Figure A1: Distribution of wives' hourly wage share around 0.5. Histogram of the wife's share of the couple's hourly wage—defined as $w_{\text{wife}}/(w_{\text{wife}} + w_{\text{husband}})$—for married, spouse-present couples with both partners aged 18–64. Sample restricted to shares in (0.20, 0.80); observations within ±0.01 of 0.50 excluded. Bars are weighted by ATUS person weights and shown as true densities (bin width = 0.01)..

C Relative earnings and family beliefs

Additional stylised facts can be drawn from the *Family and Changing Gender Roles IV* module of the ISSP survey described in ISSP Research Group (2016). Respondents report their earnings relative to their spouse on a seven-point scale ranging from "My spouse/partner has no income" to "I have no income" and express agreement with six statements on family norms, such as "A preschool child is likely to suffer when the mother works" and "Family life suffers when a woman has a full-time job."[17]

Restricting the sample to U.S. couples and excluding the extreme points of the earnings distribution[18], We can estimate

$$\text{Belief}_i = \alpha + \sum \beta, \text{RelEarn}_i + \mu X_i + \varepsilon_i, \tag{15}$$

where the dependent variable is the agreement score for a given family-norm statement; RelEarn_i is a vector of dummies indicating the wife's earnings position relative to her husband; and X_i controls for respondent sex, both spouses' ages and education levels, and

[17] Two additional items—"Being a housewife is as fulfilling as working for pay" and "Both partners should contribute to household income"—were dropped because their directional interpretation is ambiguous.

[18] Including them strengthens the dynamics, but may capture involuntarily unemployed individuals.

marriage duration. Standard errors are clustered by respondent and spouse education. Appendix Figure A2 presents the resulting marginal-effects plots.

Across statements, a distinct non-linearity emerges. For items stressing the disadvantages of maternal employment or endorsing traditional spousal roles, agreement follows an inverse-U pattern: respondents move from agreement when the wife earns far less, to disagreement near earnings parity, then back toward agreement once the wife clearly out-earns the husband. By contrast, attitudes toward maternal employment during a child's school years trace a U-shape, and responses on preschool-age children display a weaker pattern.

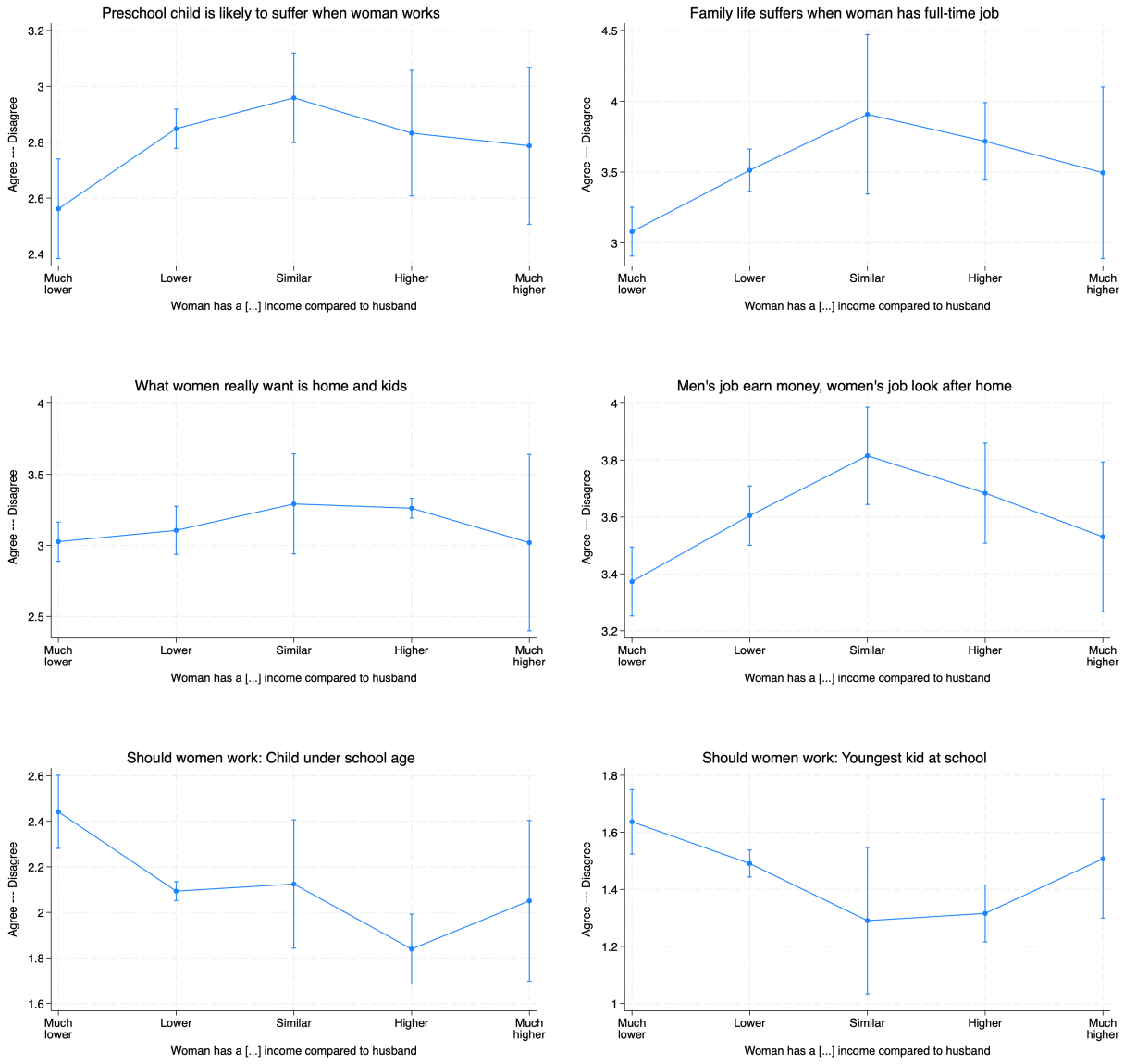

Figure A2: Marginal effects of the wife earning more than the husband on agreement with family-norm statements.

D Solution of the semi-cooperative model

The Lagrangian of the second stage problem is:

$$L_i = \delta_i \log\big(c\big) \;+\; \mu_i \log\big(1-(t_i+\tilde{t})\,n-h_i\big) \;+\; \gamma_i \log\big(n\,(1+t_i)^{\alpha}\,(1+t_{-i})^{1-\alpha}\big) \;+\; \eta\,t_i \;+\; \sigma\,t_{-i}$$

where η and σ are the Kuhn-Tucker multipliers associated to the non-negativity constraints on childcare time. The optimal solution satisfies $\eta t_f = \sigma t_m = 0$. The Nash Equilibrium of the second stage of the game can be in four regions, namely: $(\eta > 0, \sigma > 0), (\eta = 0, \sigma = 0), (\eta > 0, \sigma = 0), (\eta = 0, \sigma > 0)$.

The Lagrangian for the maximization of the first stage problem is

$$\begin{aligned} L = \theta\big(\delta_f \log(c) + \mu_f \log\big(1-(t_f+\tilde{t})\,n-h_f\big) + \gamma_f \log\big(n\,(1+t_f)^{\alpha}\,(1+t_m)^{1-\alpha}\big)\big) \\ +(1-\theta)\big(\delta_m \log(c) + \mu_m \log\big(1-(t_m+\tilde{t}m)\,n-h_m\big) \\ +\gamma_m \log\big(n\,(1+t_f)^{\alpha}\,(1+t_m)^{1-\alpha}\big)\big) + \tau\,h_f + \nu\,h_m, \end{aligned}$$

where τ and ν are the Kuhn-Tucker multipliers associated to the non-negativity constraints on working time. The optimal solution satisfies $\tau h_f = \nu h_m = 0$, with the exception of the case $h_f = h_m = 0$. We get three possible solutions for each of the four regions defined in the second stage, for a total of 12 possible time allocation regimes, listed below.

Regime 1a: $\eta > 0, \sigma > 0, \tau = 0, \nu = 0$

$$h_m = \frac{\begin{array}{l}\Big((\theta-1)nw_f + (1-\theta)\phi n\Big)\tilde{t}_f + (1-\theta)w_f + (\theta-1)\phi\Big)\,\mu_m \\ +\big(\theta n w_m \tilde{t}_m - \theta w_m\big)\,\mu_f \\ +\Big((1-\theta)nw_m\tilde{t}_m + (\theta-1)w_m\Big)\,\delta_m \\ +\big(\theta n w_m \tilde{t}_m - \theta w_m\big)\,\delta_f\end{array}}{(\theta-1)w_m\,\mu_m - \theta w_m\,\mu_f + (\theta-1)w_m\,\delta_m - \theta w_m\,\delta_f}$$

$$h_f = -\frac{\begin{array}{r}\Big((\theta-1)nw_f+(1-\theta)\phi n\Big)\tilde{t}_f+(1-\theta)w_f+(\theta-1)\phi\Big)\,\mu_m \\ +\left(\theta n w_m\tilde{t}_m-\theta w_m\right)\mu_f \\ +\Big((\theta-1)nw_f+(1-\theta)\phi n\Big)\tilde{t}_f+(1-\theta)w_f+(\theta-1)\phi\Big)\,\delta_m \\ +\Big((\theta\phi n-\theta n w_f)\tilde{t}_f+\theta w_f-\theta\phi\Big)\,\delta_f\end{array}}{\begin{array}{r}\Big((\theta-1)w_f+(1-\theta)\phi\Big)\mu_m+(\theta\phi-\theta w_f)\mu_f \\ +\Big((\theta-1)w_f+(1-\theta)\phi\Big)\delta_m+(\theta\phi-\theta w_f)\delta_f\end{array}}$$

$$t_m = 0$$

$$t_f = 0$$

Regime 1b: $\eta > 0, \sigma > 0, \tau = 0, \nu > 0$

$$h_m = 0$$

$$h_f = \frac{\left((\theta-1)n\tilde{t}_f-\theta+1\right)\delta_m+\left(\theta-\theta n\tilde{t}_f\right)\delta_f}{\theta\,\mu_f+(1-\theta)\delta_m+\theta\delta_f}$$

$$t_m = 0$$

$$t_f = 0$$

Regime 1c: $\eta > 0, \sigma > 0, \tau > 0, \nu = 0$

$$h_m = -\frac{\left((\theta-1)n\tilde{t}_m-\theta+1\right)\delta_m+\left(\theta-\theta n\tilde{t}_m\right)\delta_f}{(\theta-1)\mu_m+(\theta-1)\delta_m-\theta\delta_f}$$

$$h_f = 0$$

$$t_m = 0$$

$$t_f = 0$$

Regime 2a: $\eta = 0, \sigma = 0, \tau = 0, \nu = 0$

$$
\begin{aligned}
h_m = \frac{
&\Big((\theta-1)nw_f + (1-\theta)\phi n\Big)\tilde{t}_f + \big((1-\theta)n - \theta + 1\big)w_f + (\theta-1)\phi n + (\theta-1)\phi\Big)\,\mu_m \\
&+ \Big(\theta n w_m \tilde{t}_m + (-\theta n - \theta)w_m\Big)\,\mu_f \\
&+ \Big((1-\theta)n w_m \tilde{t}_m + \big((\theta-1)n + \theta - 1\big)w_m\Big)\,\delta_m \\
&+ \Big(\theta n w_m \tilde{t}_m + (-\theta n - \theta)w_m\Big)\,\delta_f \\
&+ \Big((\alpha - \alpha\theta)n w_m \tilde{t}_m + \big((1-\alpha)\theta + \alpha - 1\big)n w_f \tilde{t}_f + \big((\alpha-1)\theta - \alpha + 1\big)\phi n \tilde{t}_f \\
&\quad + (\alpha\theta - \alpha)n w_m + \big(((\alpha-1)\theta - \alpha + 1)n + (\alpha-1)\theta - \alpha + 1\big)w_f \\
&\quad + \big((1-\alpha)\theta + \alpha - 1\big)\phi n + \big((1-\alpha)\theta + \alpha - 1\big)\phi\Big)\gamma_m \\
&+ \Big(\alpha\theta n w_m \tilde{t}_m + \big((\alpha-1)\theta n w_f + (1-\alpha)\theta\phi n\big)\tilde{t}_f \\
&\quad + (-\alpha\theta n - \alpha\theta)w_m + \big((1-\alpha)\theta n + (1-\alpha)\theta\big)w_f + (\alpha-1)\theta\phi n + (\alpha-1)\theta\phi\Big)\gamma_f
\end{aligned}
}{
\begin{aligned}
&(\theta-1)w_m\,\mu_m - \theta w_m\,\mu_f + (\theta-1)w_m\,\delta_m - \theta w_m\,\delta_f \\
&\qquad + (\theta-1)w_m\,\gamma_m - \theta w_m\,\gamma_f
\end{aligned}
}
$$

$$
\begin{aligned}
h_f = -\,\Big(&\Big((\theta-1)nw_f+(1-\theta)\phi n\Big)\tilde{t}_f+\big((1-\theta)n-\theta+1\big)w_f+(\theta-1)\phi n+(\theta-1)\phi\Big)\,\mu_m\\
&+\Big(\theta n w_m\tilde{t}_m+(-\theta n-\theta)w_m\Big)\,\mu_f\\
&+\Big((\theta-1)nw_f+(1-\theta)\phi n\Big)\tilde{t}_f+\big((1-\theta)n-\theta+1\big)w_f+(\theta-1)\phi n+(\theta-1)\phi\Big)\,\delta_m\\
&+\Big((\theta\phi n-\theta n w_f)\tilde{t}_f+(\theta n+\theta)w_f-\theta\phi n-\theta\phi\Big)\,\delta_f\\
&+\Big((\alpha-\alpha\theta)nw_m\tilde{t}_m+\big((1-\alpha)\theta+\alpha-1\big)nw_f\tilde{t}_f+\big((\alpha-1)\theta-\alpha+1\big)\phi n\tilde{t}_f\\
&\quad+(\alpha\theta-\alpha)nw_m+\big(((\alpha-1)\theta-\alpha+1)n+(\alpha-1)\theta-\alpha+1\big)w_f\\
&\quad+\big((1-\alpha)\theta+\alpha-1\big)\phi n+\big((1-\alpha)\theta+\alpha-1\big)\phi\Big)\gamma_m\\
&+\Big(\alpha\theta n w_m\tilde{t}_m+\big((\alpha-1)\theta n w_f+(1-\alpha)\theta\phi n\big)\tilde{t}_f\\
&\quad+(-\alpha\theta n-\alpha\theta)w_m+\big((1-\alpha)\theta n+(1-\alpha)\theta\big)w_f+(\alpha-1)\theta\phi n+(\alpha-1)\theta\phi\Big)\gamma_f\Big)\\
&\Big/\Big((\theta-1)w_f+(1-\theta)\phi\Big)\mu_m+(\theta\phi-\theta w_f)\mu_f\\
&\quad+\Big((\theta-1)w_f+(1-\theta)\phi\Big)\delta_m+(\theta\phi-\theta w_f)\delta_f\\
&\quad+\Big((\theta-1)w_f+(1-\theta)\phi\Big)\gamma_m+(\theta\phi-\theta w_f)\gamma_f
\end{aligned}
$$

$$
\begin{aligned}
&(\theta-1)nw_m\,\mu_m^2\\
&+\Big(-\theta nw_m\,\mu_f+(\theta-1)nw_m\,\delta_m-\theta nw_m\,\delta_f\\
&\quad+\Big(((1-\alpha)\theta+\alpha-1)nw_m\tilde{t}_m+((1-\alpha)\theta+\alpha-1)nw_f\tilde{t}_f\\
&\qquad+\big((\alpha-1)\theta-\alpha+1\big)\phi n\tilde{t}_f+\big((\theta-1)n+(\alpha-1)\theta-\alpha+1\big)w_m\\
&\qquad+\big(((\alpha-1)\theta-\alpha+1)n+(\alpha-1)\theta-\alpha+1\big)w_f\\
&\qquad+\big((1-\alpha)\theta+\alpha-1\big)\phi n+\big((1-\alpha)\theta+\alpha-1\big)\phi\Big)\gamma_m-\theta nw_m\,\gamma_f\Big)\mu_m\\
&+\alpha-1)\theta nw_m\,\gamma_m\,\mu_f\\
&+\big((1-\alpha)\theta+\alpha-1\big)nw_m\,\gamma_m\,\delta_m+(\alpha-1)\theta nw_m\,\gamma_m\,\delta_f\\
&+\Big(((\alpha^2-2\alpha+1)\theta-\alpha^2+2\alpha-1)nw_m\tilde{t}_m\\
&\quad+((\alpha^2-2\alpha+1)\theta-\alpha^2+2\alpha-1)nw_f\tilde{t}_f\\
&\quad+\big((-\alpha^2+2\alpha-1)\theta+\alpha^2-2\alpha+1\big)\phi n\tilde{t}_f\\
&\quad+\big(((\alpha-\alpha^2)\theta+\alpha^2-\alpha)n+(-\alpha^2+2\alpha-1)\theta+\alpha^2-2\alpha+1\big)w_m\\
&\quad+\big((-\alpha^2+2\alpha-1)\theta n+(-\alpha^2+2\alpha-1)\theta\big)w_f\\
&\quad+\big((\alpha^2-2\alpha+1)\theta-\alpha^2+2\alpha-1\big)\phi n+\big((\alpha^2-2\alpha+1)\theta-\alpha^2+2\alpha-1\big)\phi\Big)\gamma_m^2\\
&+\Big((-\alpha^2+2\alpha-1)\theta nw_m\tilde{t}_m+\big((-\alpha^2+2\alpha-1)\theta nw_f+(\alpha^2-2\alpha+1)\theta\phi n\big)\tilde{t}_f\\
&\quad+\big((\alpha^2-\alpha)\theta n+(\alpha^2-2\alpha+1)\theta\big)w_m+\big((\alpha^2-2\alpha+1)\theta n+(\alpha^2-2\alpha+1)\theta\big)w_f\\
&\quad+(-\alpha^2+2\alpha-1)\theta\phi n+(-\alpha^2+2\alpha-1)\theta\phi\Big)\gamma_f\gamma_m
\end{aligned}
$$

$$
t_m=-\frac{
\begin{aligned}
&(\theta-1)nw_m\,\mu_m^2\\
&+\Big(-\theta nw_m\,\mu_f+(\theta-1)nw_m\,\delta_m-\theta nw_m\,\delta_f\\
&\quad+\big((2-2\alpha)\theta+2\alpha-2\big)nw_m\,\gamma_m-\theta nw_m\,\gamma_f\Big)\mu_m\\
&+\alpha-1)\theta nw_m\,\gamma_m\,\mu_f\\
&+\big((1-\alpha)\theta+\alpha-1\big)nw_m\,\gamma_m\,\delta_m+(\alpha-1)\theta nw_m\,\gamma_m\,\delta_f\\
&+\big((\alpha^2-2\alpha+1)\theta-\alpha^2+2\alpha-1\big)nw_m\,\gamma_m^2\\
&+\big(-\alpha^2+2\alpha-1\big)\theta nw_m\,\gamma_f\gamma_m
\end{aligned}
}{}
$$

$$
t_f = -\frac{\begin{array}{l}
\big((\theta-1)nw_f+(1-\theta)\phi n\big)\mu_f\,\mu_m+\big((\alpha\theta-\alpha)nw_f+(\alpha-\alpha\theta)\phi n\big)\gamma_f\mu_m\\
+\big(\theta\phi n-\theta nw_f\big)\mu_f^2\\
+\big((\theta-1)nw_f+(1-\theta)\phi n\big)\delta_m+\big(\theta\phi n-\theta nw_f\big)\delta_f\\
+\big((\alpha\theta-\alpha)nw_f+(\alpha-\alpha\theta)\phi n\big)\gamma_m\\
+\Big(-\alpha\theta nw_m\tilde{t}_m+(\alpha\theta\phi n-\alpha\theta nw_f)\tilde{t}_f+\alpha\theta w_m+(\alpha\theta-\alpha\theta n)w_f+\alpha\theta\phi n-\alpha\theta\phi\Big)\gamma_f\\
+\big((\alpha\theta-\alpha)nw_f+(\alpha-\alpha\theta)\phi n\big)\gamma_f\delta_m+\big(\alpha\theta\phi n-\alpha\theta nw_f\big)\gamma_f\delta_f\\
+\Big((\alpha^2\theta-\alpha^2)nw_m\tilde{t}_m+\big((\alpha^2\theta-\alpha^2)nw_f\\
+(\alpha^2-\alpha^2\theta)\phi n\big)\tilde{t}_f+(\alpha^2-\alpha^2\theta)(w_m+w_f)+(\alpha^2\theta-\alpha^2)\phi\Big)\gamma_f\gamma_m\\
+\Big(-\alpha^2\theta nw_m\tilde{t}_m+(\alpha^2\theta\phi n-\alpha^2\theta nw_f)\tilde{t}_f+\alpha^2\theta(w_m+w_f)-\alpha^2\theta\phi\Big)\gamma_f^2
\end{array}}{\begin{array}{l}
\big((\theta-1)nw_f+(1-\theta)\phi n\big)\mu_f\,\mu_m+\big((\alpha\theta-\alpha)nw_f+(\alpha-\alpha\theta)\phi n\big)\gamma_f\mu_m\\
+\big(\theta\phi n-\theta nw_f\big)\mu_f^2\\
+\big((\theta-1)nw_f+(1-\theta)\phi n\big)\delta_m+\big(\theta\phi n-\theta nw_f\big)\delta_f\\
+\big((\alpha\theta-\alpha)nw_f+(\alpha-\alpha\theta)\phi n\big)\gamma_m\\
+\big(2\alpha\theta\phi n-2\alpha\theta nw_f\big)\gamma_f\\
+\big((\alpha\theta-\alpha)nw_f+(\alpha-\alpha\theta)\phi n\big)\gamma_f\delta_m+\big(\alpha\theta\phi n-\alpha\theta nw_f\big)\gamma_f\delta_f\\
+\big((\alpha\theta-\alpha)nw_f+(\alpha-\alpha\theta)\phi n\big)\gamma_f\gamma_m+\big(\alpha\theta\phi n-\alpha\theta nw_f\big)\gamma_f^2
\end{array}}
$$

Regime 2b: $\eta=0,\sigma=0,\tau=0,\nu>0$

$$
h_m = 0
$$

$$
h_f = \frac{\big((\theta-1)n\tilde{t}_f+(1-\theta)n-\theta+1\big)\,\delta_m+\big(-\theta n\tilde{t}_f+\theta n+\theta\big)\,\delta_f}{\theta\,\mu_f+(1-\theta)\delta_m+\theta\delta_f+(\alpha-\alpha\theta)\gamma_m+\alpha\theta\gamma_f}
$$

$$
t_m = -\frac{n\,\mu_m+\big((1-\alpha)n\tilde{t}_m+\alpha-1\big)\gamma_m}{n\,\mu_m+(1-\alpha)n\,\gamma_m}
$$

$$
t_f = -\frac{\begin{array}{l}\theta n\,\mu_f^2 \\ \quad + \Big((1-\theta)n\,\delta_m + \theta n\,\delta_f + (\alpha-\alpha\theta)n\,\gamma_m + (\alpha\theta n\tilde{t}_f + \alpha\theta n - \alpha\theta)\gamma_f\Big)\mu_f \\ \quad + \big(\alpha-\alpha\theta\big)n\,\gamma_f\,\delta_m + \alpha\theta n\,\gamma_f\,\delta_f \\ \quad + \Big((\alpha^2-\alpha^2\theta)n\tilde{t}_f + \alpha^2\theta - \alpha^2\Big)\gamma_f\gamma_m + \big(\alpha^2\theta n\tilde{t}_f - \alpha^2\theta\big)\gamma_f^2\end{array}}{\begin{array}{l}\theta n\,\mu_f^2 \\ \quad + \Big((1-\theta)n\,\delta_m + \theta n\,\delta_f + (\alpha-\alpha\theta)n\,\gamma_m + 2\alpha\theta n\,\gamma_f\Big)\mu_f \\ \quad + \big(\alpha-\alpha\theta\big)n\,\gamma_f\,\delta_m + \alpha\theta n\,\gamma_f\,\delta_f \\ \quad + \big(\alpha^2-\alpha^2\theta\big)n\,\gamma_f\gamma_m + \alpha^2\theta n\,\gamma_f^2\end{array}}
$$

Regime 2c: $\eta = 0, \sigma = 0, \tau > 0, \nu = 0$

$$
h_m = -\frac{\big((\theta-1)n\tilde{t}_m + (1-\theta)n - \theta + 1\big)\,\delta_m + \big(-\theta n\tilde{t}_m + \theta n + \theta\big)\,\delta_f}{(\theta-1)\mu_m + (\theta-1)\delta_m - \theta\delta_f + ((1-\alpha)\theta + \alpha - 1)\gamma_m + (\alpha-1)\theta\gamma_f}
$$

$$
h_f = 0
$$

$$
t_m = -\frac{\begin{array}{l}(\theta-1)n\,\mu_m^2 \\ \quad + \Big((\theta-1)n\,\delta_m - \theta n\,\delta_f + \big(((1-\alpha)\theta + \alpha - 1)n\tilde{t}_m \\ \quad + ((1-\alpha)\theta + \alpha - 1)n + (\alpha-1)\theta - \alpha + 1\big)\gamma_m \quad + (\alpha-1)\theta n\,\gamma_f\Big)\mu_m \\ \quad + \big((1-\alpha)\theta + \alpha - 1\big)n\gamma_m\,\delta_m + (\alpha-1)\theta n\gamma_m\,\delta_f \\ \quad + \Big(((\alpha^2-2\alpha+1)\theta - \alpha^2 + 2\alpha - 1)n\tilde{t}_m + (-\alpha^2+2\alpha-1)\theta + \alpha^2 - 2\alpha + 1\Big)\gamma_m^2 \\ \quad + \Big((-\alpha^2+2\alpha-1)\theta n\tilde{t}_m + (\alpha^2-2\alpha+1)\theta\Big)\gamma_f\gamma_m\end{array}}{\begin{array}{l}(\theta-1)n\,\mu_m^2 \\ \quad + \Big((\theta-1)n\,\delta_m - \theta n\,\delta_f + \big((2-2\alpha)\theta + 2\alpha - 2\big)n\gamma_m + (\alpha-1)\theta n\,\gamma_f\Big)\mu_m \\ \quad + \big((1-\alpha)\theta + \alpha - 1\big)n\gamma_m\,\delta_m + (\alpha-1)\theta n\gamma_m\,\delta_f \\ \quad + \big((\alpha^2-2\alpha+1)\theta - \alpha^2 + 2\alpha - 1\big)n\gamma_m^2 + (-\alpha^2+2\alpha-1)\theta n\,\gamma_f\gamma_m\end{array}}
$$

$$
t_f = -\frac{n\,\mu_f + (\alpha n\tilde{t}_f - \alpha)\gamma_f}{n\,\mu_f + \alpha n\,\gamma_f}
$$

Regime 3a: $\eta > 0, \sigma = 0, \tau = 0, \nu = 0$

$$h_m = \frac{\begin{array}{l}\Big((\theta-1)nw_f + (1-\theta)\phi n\Big)\tilde{t}_f + (1-\theta)w_f + (\theta-1)\phi\Big)\,\mu_m \\ + \Big(\theta n w_m \tilde{t}_m + (-\theta n - \theta)w_m\Big)\,\mu_f \\ + \Big((1-\theta)nw_m\tilde{t}_m + \big((\theta-1)n + \theta - 1\big)w_m\Big)\,\delta_m \\ + \Big(\theta n w_m \tilde{t}_m + (-\theta n - \theta)w_m\Big)\,\delta_f \\ + \Big(\big((1-\alpha)\theta + \alpha - 1\big)nw_f + \big((\alpha-1)\theta - \alpha + 1\big)\phi n\Big)\tilde{t}_f \\ + \big((\alpha-1)\theta - \alpha + 1\big)w_f + \big((1-\alpha)\theta + \alpha - 1\big)\phi\Big)\,\gamma_m \\ + \Big(\big((\alpha-1)\theta n w_f + (1-\alpha)\theta\phi n\big)\tilde{t}_f + (1-\alpha)\theta w_f + (\alpha-1)\theta\phi\Big)\,\gamma_f\end{array}}{\begin{array}{l}(\theta-1)w_m\,\mu_m - \theta w_m\,\mu_f \\ + \big((\theta-1)w_m - \theta w_m\big)\delta_m - \theta w_m\,\delta_f \\ + \big((1-\alpha)\theta + \alpha - 1\big)w_m\,\gamma_m + (\alpha-1)\theta w_m\,\gamma_f\end{array}}$$

$$h_f = -\frac{\begin{array}{l}\Big((\theta-1)nw_f + (1-\theta)\phi n\Big)\tilde{t}_f + (1-\theta)w_f + (\theta-1)\phi\Big)\,\mu_m \\ + \Big(\theta n w_m \tilde{t}_m + (-\theta n - \theta)w_m\Big)\,\mu_f \\ + \Big((\theta-1)nw_f + (1-\theta)\phi n\Big)\tilde{t}_f + (1-\theta)w_f + (\theta-1)\phi\Big)\,\delta_m \\ + \Big((\theta\phi n - \theta n w_f)\tilde{t}_f + \theta w_f - \theta\phi\Big)\,\delta_f \\ + \Big(\big((1-\alpha)\theta + \alpha - 1\big)nw_f + \big((\alpha-1)\theta - \alpha + 1\big)\phi n\Big)\tilde{t}_f + \big((\alpha-1)\theta - \alpha + 1\big)w_f + \big((1-\alpha)\theta \\ + \alpha - 1\big)\phi\Big)\,\gamma_m + \Big(\big((\alpha-1)\theta n w_f + (1-\alpha)\theta\phi n\big)\tilde{t}_f + (1-\alpha)\theta w_f + (\alpha-1)\theta\phi\Big)\,\gamma_f\end{array}}{\begin{array}{l}\Big((\theta-1)w_f + (1-\theta)\phi\Big)\mu_m + (\theta\phi - \theta w_f)\mu_f \\ + \Big((\theta-1)w_f + (1-\theta)\phi\Big)\delta_m + (\theta\phi - \theta w_f)\delta_f \\ + \big((1-\alpha)\theta + \alpha - 1\big)w_f + \big((\alpha-1)\theta - \alpha + 1\big)\phi\Big)\gamma_m \\ + \big((\alpha-1)\theta w_f + (1-\alpha)\theta\phi\big)\gamma_f\end{array}}$$

$$
t_m = -\frac{
\begin{aligned}
&(\theta-1)nw_m\,\mu_m^2 \\
&+\Big(-\theta nw_m\,\mu_f+(\theta-1)nw_m\,\delta_m-\theta nw_m\,\delta_f \\
&\quad+\Big(((1-\alpha)\theta+\alpha-1)nw_m\tilde{t}_m+((1-\alpha)\theta+\alpha-1)nw_f\tilde{t}_f \\
&\qquad+\big((\alpha-1)\theta-\alpha+1\big)\phi n\tilde{t}_f+\big(((1-\theta)+\alpha-1)n+(\alpha-1)\theta-\alpha+1\big)w_m \\
&\qquad+\big((\alpha-1)\theta-\alpha+1\big)w_f+\big((1-\alpha)\theta+\alpha-1\big)\phi\Big)\gamma_m+(\alpha-1)\theta nw_m\,\gamma_f\Big)\mu_m \\
&+\big(\alpha-1\big)\theta nw_m\,\gamma_m\,\mu_f \\
&+\big((1-\alpha)\theta+\alpha-1\big)nw_m\,\gamma_m\,\delta_m+(\alpha-1)\theta nw_m\,\gamma_m\,\delta_f \\
&+\Big(((\alpha^2-2\alpha+1)\theta-\alpha^2+2\alpha-1)nw_m\tilde{t}_m \\
&\quad+((\alpha^2-2\alpha+1)\theta-\alpha^2+2\alpha-1)nw_f\tilde{t}_f \\
&\quad+\big((-\alpha^2+2\alpha-1)\theta+\alpha^2-2\alpha+1\big)\phi n\tilde{t}_f \\
&\quad+\big((-\alpha^2+2\alpha-1)\theta+\alpha^2-2\alpha+1\big)w_m \\
&\quad+\big((-\alpha^2+2\alpha-1)\theta+\alpha^2-2\alpha+1\big)w_f \\
&\quad+\big((\alpha^2-2\alpha+1)\theta-\alpha^2+2\alpha-1\big)\phi\Big)\gamma_m^2 \\
&+\Big((-\alpha^2+2\alpha-1)\theta nw_m\tilde{t}_m+\big((-\alpha^2+2\alpha-1)\theta nw_f+(\alpha^2-2\alpha+1)\theta\phi n\big)\tilde{t}_f \\
&\quad+\big((\alpha^2-2\alpha+1)\theta+\alpha^2-2\alpha+1\big)w_m \\
&\quad+\big((\alpha^2-2\alpha+1)\theta+\alpha^2-2\alpha+1\big)w_f+(-\alpha^2+2\alpha-1)\theta\phi\Big)\gamma_f\gamma_m
\end{aligned}
}{
\begin{aligned}
&(\theta-1)nw_m\,\mu_m^2 \\
&+\Big(-\theta nw_m\,\mu_f+(\theta-1)nw_m\,\delta_m-\theta nw_m\,\delta_f \\
&\quad+\big((2-2\alpha)\theta+2\alpha-2\big)nw_m\,\gamma_m+(\alpha-1)\theta nw_m\,\gamma_f\Big)\mu_m \\
&+\big(\alpha-1\big)\theta nw_m\,\gamma_m\,\mu_f \\
&+\big((1-\alpha)\theta+\alpha-1\big)nw_m\,\gamma_m\,\delta_m+(\alpha-1)\theta nw_m\,\gamma_m\,\delta_f \\
&+\big((\alpha^2-2\alpha+1)\theta-\alpha^2+2\alpha-1\big)nw_m\,\gamma_m^2+(-\alpha^2+2\alpha-1)\theta nw_m\,\gamma_f\gamma_m
\end{aligned}
}
$$

$$
t_f = 0
$$

Regime 3b: $\eta > 0, \sigma = 0, \tau = 0, \nu > 0$

$$h_m = 0$$

$$h_f = \frac{\big((\theta-1)n\tilde{t}_f - \theta + 1\big)\,\delta_m + \big(\theta - \theta n\tilde{t}_f\big)\,\delta_f}{\theta\,\mu_f + (1-\theta)\delta_m + \theta\delta_f}$$

$$t_m = -\,\frac{n\,\mu_m + \big((1-\alpha)n\tilde{t}_m + \alpha - 1\big)\gamma_m}{n\,\mu_m + (1-\alpha)n\,\gamma_m}$$

Regime 3c: $\eta > 0, \sigma = 0, \tau > 0, \nu = 0$

$$h_m = -\,\frac{\big((\theta-1)n\tilde{t}_m + (1-\theta)n - \theta + 1\big)\,\delta_m + \big(-\theta n\tilde{t}_m + \theta n + \theta\big)\,\delta_f}{(\theta-1)\mu_m + (\theta-1)\delta_m - \theta\delta_f + \big((1-\alpha)\theta + \alpha - 1\big)\gamma_m + (\alpha-1)\theta\gamma_f}$$

$$h_f = 0$$

$$t_m = -\,\frac{\begin{array}{l}(\theta-1)n\,\mu_m^2 \\ \quad + \Big((\theta-1)n\,\delta_m - \theta n\,\delta_f + \big((1-\alpha)\theta + \alpha - 1\big)n\tilde{t}_m + \big((1-\alpha)\theta + \alpha - 1\big)n \\ \qquad + (\alpha-1)\theta - \alpha + 1\Big)\gamma_m + (\alpha-1)\theta n\,\gamma_f\Big)\mu_m \\ \quad + \big((1-\alpha)\theta + \alpha - 1\big)n\gamma_m\,\delta_m + (\alpha-1)\theta n\gamma_m\,\delta_f \\ \quad + \big((\alpha^2 - 2\alpha + 1)\theta - \alpha^2 + 2\alpha - 1\big)n\tilde{t}_m + \big(-\alpha^2 + 2\alpha - 1\big)\theta + \alpha^2 - 2\alpha + 1\Big)\gamma_m^2 \\ \quad + \Big((-\alpha^2 + 2\alpha - 1)\theta n\tilde{t}_m + (\alpha^2 - 2\alpha + 1)\theta\Big)\gamma_f\gamma_m\end{array}}{\begin{array}{l}(\theta-1)n\,\mu_m^2 \\ \quad + \Big((\theta-1)n\,\delta_m - \theta n\,\delta_f + \big((2-2\alpha)\theta + 2\alpha - 2\big)n\gamma_m + (\alpha-1)\theta n\,\gamma_f\Big)\mu_m \\ \quad + \big((1-\alpha)\theta + \alpha - 1\big)n\gamma_m\,\delta_m + (\alpha-1)\theta n\gamma_m\,\delta_f \\ \quad + \big((\alpha^2 - 2\alpha + 1)\theta - \alpha^2 + 2\alpha - 1\big)n\gamma_m^2 + \big(-\alpha^2 + 2\alpha - 1\big)\theta n\,\gamma_f\gamma_m\end{array}}$$

$$t_f = 0$$

Regime 4a: $\eta = 0, \sigma > 0, \tau = 0, \nu = 0$

$$
\begin{aligned}
h_m = \frac{}{}
&\Big((\theta-1)nw_f + (1-\theta)\phi n\Big)\tilde{t}_f + \big((1-\theta)n - \theta + 1\big)w_f + (\theta-1)\phi n + (\theta-1)\phi\Big)\,\mu_m \\
&+ \big(\theta n w_m \tilde{t}_m - \theta w_m\big)\,\mu_f \\
&+ \Big((1-\theta)nw_m\tilde{t}_m + (\theta-1)w_m\Big)\,\delta_m \\
&+ \big(\theta n w_m \tilde{t}_m - \theta w_m\big)\,\delta_f \\
&+ \Big((\alpha-\alpha\theta)nw_m\tilde{t}_m + (\alpha\theta-\alpha)w_m\Big)\,\gamma_m \\
&+ \Big(\alpha\theta n w_m \tilde{t}_m - \alpha\theta w_m\Big)\,\gamma_f \\
\hline
&(\theta-1)w_m\,\mu_m - \theta w_m\,\mu_f + (\theta-1)w_m\,\delta_m - \theta w_m\,\delta_f \\
&\qquad +(\alpha\theta-\alpha)w_m\,\gamma_m - \alpha\theta w_m\,\gamma_f
\end{aligned}
$$

$$
\begin{aligned}
h_f = -\frac{}{}
&\Big((\theta-1)nw_f + (1-\theta)\phi n\Big)\tilde{t}_f + \big((1-\theta)n - \theta + 1\big)w_f + (\theta-1)\phi n + (\theta-1)\phi\Big)\,\mu_m \\
&+ \big(\theta n w_m \tilde{t}_m - \theta w_m\big)\,\mu_f \\
&+ \Big((\theta-1)nw_f + (1-\theta)\phi n\Big)\tilde{t}_f + \big((1-\theta)n - \theta + 1\big)w_f + (\theta-1)\phi n + (\theta-1)\phi\Big)\,\delta_m \\
&+ \Big((\theta\phi n - \theta n w_f)\tilde{t}_f + (\theta n + \theta)w_f - \theta\phi n - \theta\phi\Big)\,\delta_f \\
&+ \Big((\alpha-\alpha\theta)nw_m\tilde{t}_m + (\alpha\theta-\alpha)w_m\Big)\,\gamma_m \\
&+ \Big(\alpha\theta n w_m \tilde{t}_m - \alpha\theta w_m\Big)\,\gamma_f \\
\hline
&\Big((\theta-1)w_f + (1-\theta)\phi\Big)\mu_m + (\theta\phi - \theta w_f)\mu_f \\
&\quad + \Big((\theta-1)w_f + (1-\theta)\phi\Big)\delta_m + (\theta\phi - \theta w_f)\delta_f \\
&\quad + \Big((\alpha\theta-\alpha)w_f + (\alpha-\alpha\theta)\phi\Big)\gamma_m + (\alpha\theta\phi - \alpha\theta w_f)\gamma_f
\end{aligned}
$$

$$t_m = 0$$

$$t_f = -\frac{\begin{array}{l}\Big((\theta-1)nw_f+(1-\theta)\phi n\Big)\mu_f+\Big((\alpha\theta-\alpha)nw_f+(\alpha-\alpha\theta)\phi n\Big)\gamma_f\Big)\mu_m\\ +\big(\theta\phi n-\theta nw_f\big)\mu_f^2\\ +\Big((\theta-1)nw_f+(1-\theta)\phi n\Big)\delta_m+\big(\theta\phi n-\theta nw_f\big)\delta_f\\ +\Big((\theta-1)nw_f+(1-\theta)\phi n\Big)\gamma_m\\ +\Big(-\alpha\theta nw_m\tilde{t}_m+(\alpha\theta\phi n-\alpha\theta nw_f)\tilde{t}_f+(\alpha\theta n+\alpha\theta)w_m+(\alpha\theta-\theta n)w_f+\theta\phi n-\alpha\theta\phi\Big)\gamma_f\\ +\big((\alpha\theta-\alpha)nw_f+(\alpha-\alpha\theta)\phi n\big)\gamma_f\delta_m+\big(\alpha\theta\phi n-\alpha\theta nw_f\big)\gamma_f\delta_f\\ +\Big((\alpha^2\theta-\alpha^2)nw_m\tilde{t}_m+\big((\alpha^2\theta-\alpha^2)nw_f\\ +(\alpha^2-\alpha^2\theta)\phi n\big)\tilde{t}_f+(\alpha^2-\alpha^2\theta)(w_m+w_f)+(\alpha^2\theta-\alpha^2)\phi\Big)\gamma_f\gamma_m\\ +\Big(-\alpha^2\theta nw_m\tilde{t}_m+(\alpha^2\theta\phi n-\alpha^2\theta nw_f)\tilde{t}_f+\alpha^2\theta(w_m+w_f)-\alpha^2\theta\phi\Big)\gamma_f^2\end{array}}{\begin{array}{l}\Big((\theta-1)nw_f+(1-\theta)\phi n\Big)\mu_f+\Big((\alpha\theta-\alpha)nw_f+(\alpha-\alpha\theta)\phi n\Big)\gamma_f\Big)\mu_m\\ +\big(\theta\phi n-\theta nw_f\big)\mu_f^2\\ +\Big((\theta-1)nw_f+(1-\theta)\phi n\Big)\delta_m+\big(\theta\phi n-\theta nw_f\big)\delta_f\\ +\Big((\theta-1)nw_f+(1-\theta)\phi n\Big)\gamma_m\\ +\big((-\alpha-1)\theta nw_f+(\alpha+1)\theta\phi n\big)\gamma_f\,\mu_f\\ +\big((\alpha\theta-\alpha)nw_f+(\alpha-\alpha\theta)\phi n\big)\gamma_f\delta_m+\big(\alpha\theta\phi n-\alpha\theta nw_f\big)\gamma_f\delta_f\\ +\big((\alpha\theta-\alpha)nw_f+(\alpha-\alpha\theta)\phi n\big)\gamma_f\gamma_m+\big(\alpha\theta\phi n-\alpha\theta nw_f\big)\gamma_f^2\end{array}}$$

Regime 4b: $\eta = 0, \sigma > 0, \tau = 0, \nu > 0$

$$h_m = 0$$

$$h_f = \frac{\big((\theta-1)n\tilde{t}_f+(1-\theta)n-\theta+1\big)\,\delta_m+\big(-\theta n\tilde{t}_f+\theta n+\theta\big)\,\delta_f}{\theta\,\mu_f+(1-\theta)\delta_m+\theta\delta_f+(\alpha-\alpha\theta)\gamma_m+\alpha\theta\gamma_f}$$

$$t_m = 0$$

$$t_f = -\frac{\begin{array}{l}\theta n\,\mu_f^2 + \Big((1-\theta)n\,\delta_m + \theta n\,\delta_f + (\alpha-\alpha\theta)n\,\gamma_m + (\alpha\theta n\tilde{t}_f + \alpha\theta n - \alpha\theta)\gamma_f\Big)\mu_f \\ + \big(\alpha-\alpha\theta\big)n\,\gamma_f\,\delta_m + \alpha\theta n\,\gamma_f\,\delta_f \\ + \Big((\alpha^2-\alpha^2\theta)n\tilde{t}_f + \alpha^2\theta - \alpha^2\Big)\gamma_f\gamma_m + \big(\alpha^2\theta n\tilde{t}_f - \alpha^2\theta\big)\gamma_f^2\end{array}}{\begin{array}{l}\theta n\,\mu_f^2 + \Big((1-\theta)n\,\delta_m + \theta n\,\delta_f + (\alpha-\alpha\theta)n\,\gamma_m + 2\alpha\theta n\,\gamma_f\Big)\mu_f \\ + \big(\alpha-\alpha\theta\big)n\,\gamma_f\,\delta_m + \alpha\theta n\,\gamma_f\,\delta_f \\ + \big(\alpha^2-\alpha^2\theta\big)n\,\gamma_f\gamma_m + \alpha^2\theta n\,\gamma_f^2\end{array}}$$

Regime 4c: $\eta = 0, \sigma > 0, \tau > 0, \nu = 0$

$$h_m = -\frac{\big((\theta-1)n\tilde{t}_m - \theta + 1\big)\,\delta_m + \big(\theta - \theta n\tilde{t}_m\big)\,\delta_f}{(\theta-1)\mu_m + (\theta-1)\delta_m - \theta\delta_f}$$

$$h_f = 0$$

$$t_m = 0$$

$$t_f = -\frac{n\,\mu_f + (\alpha n\tilde{t}_f - \alpha)\gamma_f}{n\,\mu_f + \alpha n\,\gamma_f}$$

D.1 Proof of Proposition 1

Stage 2. Fix (h_f, h_m). Player i solves a strictly concave problem in t_i:

$$v_i(t_i; t_{-i}, h_f, h_m) = \log(c) + \mu_i \log\big(1 - h_i - (t_i + \tilde{t}_i)n\big) + \gamma_i \log\big((1+t_f)^\alpha (1+t_m)^{1-\alpha} n\big),$$

over a nonempty, convex, compact interval for t_i (A3). The second derivative in own strategy,

$$\frac{\partial^2 v_i}{\partial t_i^2} = -\frac{\mu_i n^2}{\big(1 - h_i - (t_i + \tilde{t}_i)n\big)^2} - \frac{\gamma_i}{(1+t_i)^2} \times \begin{cases} \alpha & \text{if } i = f, \\ 1-\alpha & \text{if } i = m, \end{cases}$$

is strictly negative, so each payoff is strictly concave in own action. The Jacobian of first-order conditions has a symmetric part whose diagonal entries dominate the off-diagonal terms (the cross–partial from $\log q$), implying diagonal strict concavity (DSC). By Rosen's (1965) theorem, a unique Nash equilibrium (t_f^*, t_m^*) exists; by the implicit function theorem and DSC, (t_f^*, t_m^*) is continuous in (h_f, h_m).

Stage 1. Define $V(h_f, h_m) = \theta v_f\big(h_f, h_m, t^*(h)\big) + (1-\theta) v_m\big(h_f, h_m, t^*(h)\big)$. The feasible set for (h_f, h_m) is convex/compact (A3). The only non-affine term in (h_f, h_m) is $\log c$ with $c = \phi(s) w_f h_f + w_m h_m$. Under A2, the mapping $(h_f, h_m) \mapsto \log c$ is strictly concave on the feasible set.[19] All remaining terms in V are (strictly) concave in (h_f, h_m), and composition with the single-valued continuous correspondence $t^*(h)$ preserves concavity. Hence V is strictly concave and attains a unique maximizer (h_f^*, h_m^*). Combining with the unique (t_f^*, t_m^*) from Stage 2 yields a unique subgame-perfect equilibrium.

□

[19] For $\phi(s) = \exp[-\chi s^\kappa]$ with $s = \frac{w_f h_f}{w_f h_f + w_m h_m}$ the Hessian of $\log c$ is negative definite whenever $\chi \leq \bar{\chi}(\kappa, w_f, w_m, \underline{h}, \overline{h})$; an explicit bound is obtained by comparing $|\partial^2 \log c / \partial h_i \partial h_j|$ with the diagonal terms and using the fact that $h_i \in [\underline{h}, \overline{h}]$. If s is defined on *potential* shares $w_f/(w_f + w_m)$, $\log c$ is strictly concave without any restriction on χ.